

Decoupled Reference Governors: A Constraint Management Technique for MIMO Systems

Yudan Liu^a, Joycer Osorio^b, Hamid R. Ossareh^c

^{a,b,c}Department of Electrical and Biomedical Engineering, University Of Vermont, Burlington, VT USA

ARTICLE HISTORY

Compiled December 4, 2020

Abstract

This paper presents a computationally efficient solution for constraint management of multi-input and multi-output (MIMO) systems. The solution, referred to as the Decoupled Reference Governor (DRG), maintains the highly-attractive computational features of Scalar Reference Governors (SRG) while having performance comparable to Vector Reference Governors (VRG). DRG is based on decoupling the input-output dynamics of the system, followed by the deployment of a bank of SRGs for each decoupled channel. We present two formulations of DRG: DRG-tf, which is based on system decoupling using transfer functions, and DRG-ss, which is built on state feedback decoupling. A detailed set-theoretic analysis of DRG, which highlights its main characteristics, is presented. We also show a quantitative comparison between DRG and the VRG to illustrate the computational advantages of DRG. The robustness of this approach to disturbances and uncertainties is also investigated.

KEYWORDS

Constraint management; Reference governors; Maximal admissible set; System decoupling; MIMO systems

1. Introduction

Control and constraint management of systems with multiple inputs and multiple outputs (i.e., MIMO systems) have been studied in the field of controls for many decades. The control of MIMO systems has been the focus of many works in the literature, for example the Linear Quadratic Regulator (LQR), state feedback control methods, sliding mode control, \mathcal{H}_2 and \mathcal{H}_∞ control, and decentralized and centralized control methods, please see **Skogestad'2007**; Burl, 1998; Garelli et al., 2006; Ge and Li, 2014; Zhou et al., 1996 and the references therein. The problem of constraint management of MIMO systems has been explored as well. One route is to first find a suitable compensator to decouple the input-output dynamics, see **Skogestad'2007**; A. G. J. MacFarlane, 1970; A. MacFarlane and Hung, 1983. Afterwards, a diagonal controller for the newly decoupled plant is designed. The constraint management part is handled by nonlinear functions (e.g., saturation functions) that maintain the constrained signal within the desired bounds (Åström and Hägglund, 1995). However, this approach

CONTACT Yudan Liu. Email: yliu38@uvm.edu

CONTACT Joycer Osorio. Email: Joycer.Osorio@uvm.edu

CONTACT Hamid R. Ossareh. Email: Hamid.Ossareh@uvm.edu

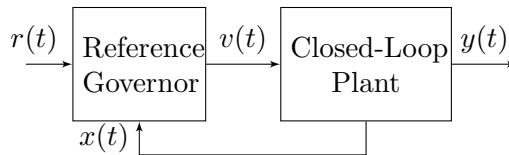


Figure 1. Scalar reference governor block diagram

can compromise the closed-loop stability and may not enforce state constraints. Another approach is Model Predictive Control (MPC), see Bemporad et al., 2002; Shah and Engell, 2011, which addresses both tracking and constraint management at the same time. This approach for constraint management in MIMO systems is explored in works like Elliott and Rasmussen, 2013, where decentralized MPC strategies are proposed. Other MPC solutions are centralized (Wenlin Wang et al., 2003), distributed (Camponogara et al., 2002), and cascade or hierarchical strategies (Scattolini, 2009). However, MPC tends to be computationally demanding, which has limited its applicability, especially for systems with fast dynamics and/or high order. Theoretical guarantees such as stability are also difficult to obtain in practice. Other approaches to solve constraint management are l_1 -optimal control, see McDonald and Pearson, 1991, barrier Lyapunov function, see Tee et al., 2009, and constrained LQR, see Scokaert and Rawlings, 1998.

A relatively new constraint management technique, which can be designed independently of the tracking controller and alleviates the above shortcomings of MPC, is the Reference Governor (Garone et al., 2017; Kolmanovsky et al., 2014), also referred to as the Scalar Reference Governor (SRG). It is an add-on scheme for enforcing pointwise-in-time state and control constraints by modifying, whenever required, the reference to a well-designed stable closed-loop system. A block diagram of SRG is shown in Figure 1, where $y(t)$ is the constrained output, $r(t)$ is the reference, $v(t)$ is the governed reference, and $x(t)$ is the system state (measured or estimated). To compute $v(t)$, SRG employs the so-called maximal admissible set (MAS) (Gilbert and Tan, 1991), which is defined as the set of all inputs and initial conditions that are constraint-admissible. By solving a simple linear program over this set, SRG selects a $v(t)$ that is as close as possible to $r(t)$ such that the constraints are satisfied for all time.

Standard SRG uses a single decision variable in the linear program to simultaneously govern all the channels of a MIMO system. As a result, it tends to have a conservative response. A modification of the SRG, which performs well in MIMO systems, is the so-called Vector Reference Governor (VRG), see Garone et al., 2017. This technique handles constraint management by solving a quadratic program (QP) with multiple decision variables (one for each reference input). Even though VRG shares some properties with SRG, its implementation demands a higher computational load in comparison with SRG. This is because of the QP with multiple decision variables that must be solved at each time step, either by implicit methods or multi-parametric explicit methods. In this paper, we present a new reference governor solution for MIMO systems that maintains the computational simplicity of the SRG, but with performance similar to VRG. The solution, referred to as the Decoupled Reference Governor (DRG), is based on decoupling the input-output dynamics of the system, followed by the deployment of a bank of SRGs for each decoupled channel. Since the decoupling operation can be performed in both transfer function and state-space domains, we investigate two DRG formulations: DRG-tf, and DRG-ss, as summarized next.

The block diagram of the DRG-tf method is shown in Figure 2, where $G(z)$ is the

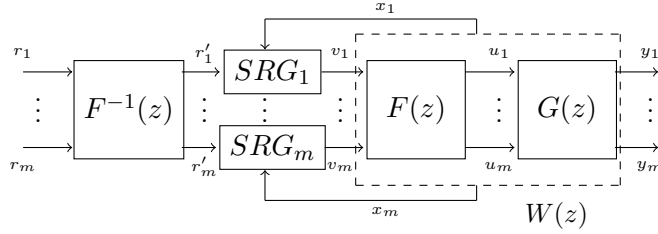


Figure 2. DRG-tf block diagram.

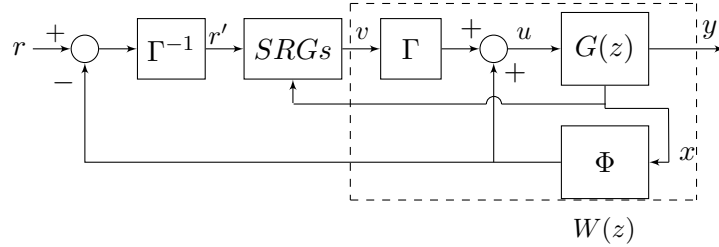


Figure 3. DRG-ss block diagram. r, r', v, u, y represent $[r_1, r_2, \dots, r_m]^T, [r'_1, r'_2, \dots, r'_m]^T, [v_1, v_2, \dots, v_m]^T, [u_1, u_2, \dots, u_m]^T$, and $[y_1, y_2, \dots, y_m]^T$, respectively.

closed-loop system with inputs u_i and constrained outputs y_i . In this block diagram, we have assumed that the system is square, i.e., it has m inputs and m outputs, because the decoupling operation can only be applied to square systems. We will extend the theory to non-square systems in Section 7, but for the ease of illustration, assume for now that $G(z)$ is a square system. Over the output, the constraints are imposed: $y_i(t) \in \mathbb{Y}_i, \forall t$, where \mathbb{Y}_i are specified sets. Given the set-points r_i , the goal is to select each u_i as close as possible to r_i (to ensure that the tracking outputs, which are not shown in the figure, follow $r_i(t)$ as closely as possible) while ensuring that the output constraints are satisfied, i.e., $y_i(t) \in \mathbb{Y}_i, \forall t$. The DRG-tf method achieves these goals as follows: first, system $G(z)$ is decoupled by finding a suitable filter, $F(z)$, that eliminates the coupling dynamics of $G(z)$. The resulting decoupled system is $W(z) := G(z)F(z)$, which is diagonal; that is, each output y_i depends only on the new input v_i . Second, we introduce a bank of m decoupled SRGs, where the goal of the i -th SRG is to select v_i as close as possible to r'_i while ensuring $y_i \in \mathbb{Y}_i$. Each SRG_i (see Figure 2) uses only the states of the i -th decoupled subsystem. Finally, since we would like to ensure that $u_i = r_i$ when r_i is constraint-admissible, we introduce the inverse of the filter, $F^{-1}(z)$, to cancel the effects of $F(z)$. Note that $F^{-1}(z)$ also ensures that u_i and r_i are close if r_i is not constraint-admissible.

Similar to DRG-tf, DRG-ss is based on decoupling the input-output dynamics as shown in Figure 3. The difference is that the system G is decoupled by using state feedback, where the feedback matrices Φ and Γ are properly chosen as will be discussed later in this paper. Second step is introducing m decoupled SRGs, whose goal is the same as the SRGs in DRG-tf. Finally, to make sure that $u_i = r_i$ when r_i is constraint-admissible, x is fed back through $\Gamma^{-1}(r - \Phi x)$.

Finally, we handle non-square systems by transforming them into square ones and applying the DRG theory explained above to the resulting square system. Detailed information will be provided in Section 7.

Because of the decoupling process, DRG-ss differs from DRG-tf in its analysis, implementation, and observer design. Furthermore, DRG-ss contains an additional feedback loop, which may compromise closed-loop stability. Thus, in this paper, we present a detailed analysis of both methods, including stability, transient and steady-state properties, and observer design considerations. We also study the class of systems for which DRG performs well, and present an analysis of the robustness of DRG to unmeasured disturbances and parametric uncertainties. Note that a preliminary exposition of DRG-tf was presented in a conference version of this paper in Liu et al., 2018. The current paper improves on Liu et al., 2018 by presenting a complete analysis of the transient and steady-state characteristics of DRG-tf, introducing and studying DRG-ss, discussing observer design considerations, presenting the robustness analysis mentioned above, and introducing the extension of DRG-tf and DRG-ss to non-square systems.

The main contributions of this research are as follows:

- A computationally efficient constraint management technique for square MIMO systems (i.e., the DRG), which is a novel extension of the SRG. Two formulations of DRG (i.e., DRG-ss and DRG-tf), and their advantages and disadvantages, are studied.
- Analysis of stability and performance of DRG in comparison with VRG. We show that the proposed approach is most suitable for a specific class of systems and illustrate this by examples.
- Quantitative comparison of explicit and implicit optimization techniques for VRG and DRG, where we show that DRG algorithm can run two orders of magnitude faster than VRG at every time step.
- A novel extension of DRG to systems that are affected by unknown additive disturbances and parametric uncertainties.
- An extension of DRG to non-square MIMO systems, which enhances the applicability of DRG.

2. Preliminaries

In this section, we introduce the notations and norms that are used in this paper. Then, we review the decoupling methods and reference governor schemes.

The following notations are used in this paper. \mathbb{Z}_+ denotes the set of all non-negative integers. Let $V, U \subset \mathbb{R}^n$. Then, $V \sim U := \{z \in \mathbb{R}^n : z + u \in V, \forall u \in U\}$ is the Pontryagin-subtraction (P-subtraction) (Kolmanovsky and Gilbert, 1998). The identity matrix with dimension $i \times i$ is denoted by I_i . Given a discrete-time signal $u(t) = [u_1(t), u_2(t), \dots, u_m(t)]^T$, the L_2 norm is defined as: $\|u\|_{L_2}^2 = \sum_{t=-\infty}^{\infty} u(t)^T u(t)$, and its L_∞ norm is represented as: $\|u(t)\|_{L_\infty} = \sup_t (\max_i |u_i(t)|)$. For a system with transfer function $F(z)$ and impulse response $f(t)$, the H_∞ norm is defined as: $\|F\|_{H_\infty} = \max_w \bar{\sigma}(F(e^{jw}))$, where $\bar{\sigma}$ represents the maximum singular value, and the L_1 norm is defined as: $\|f(t)\|_{L_1} = \max_i \sum_{j=1}^m \sum_{\tau=0}^{\infty} |f_{ij}(\tau)|$, where f_{ij} is the ij -th element of f , and m is the number of columns of f . We denote the condition number of a matrix (defined by the ratio of the maximum to the minimum singular values) by γ . A zero matrix with dimension $i \times j$ is denoted as $0_{i,j}$.

2.1. Review Of Decoupling Methods

In this section, we review two decoupling methods, one based on transfer functions (Skogestad'2007) and the other based on state space (Falb and Wolovich, 1967).

2.1.1. Decoupling Method Based on Transfer Functions

Consider the square coupled system $G(z)$ shown in Figure 2 and defined as:

$$\begin{bmatrix} Y_1(z) \\ \vdots \\ Y_m(z) \end{bmatrix} = \underbrace{\begin{bmatrix} G_{11}(z) & \dots & G_{1m}(z) \\ \vdots & \ddots & \vdots \\ G_{m1}(z) & \dots & G_{mm}(z) \end{bmatrix}}_{G(z)} \begin{bmatrix} U_1(z) \\ \vdots \\ U_m(z) \end{bmatrix} \quad (1)$$

where Y_i and U_i are the \mathcal{Z} -transforms of y_i and u_i , respectively. The system $G(z)$ consists of diagonal subsystems with dynamics $G_{ii}(z)$ and off-diagonal (interaction) subsystems with dynamics $G_{ij}(z), i \neq j$. A decoupled system is perfectly diagonal (i.e., each output depends on only one input). As shown in Figure 2, we decouple the system by adding a filter, $F(z)$, before $G(z)$, so that the product $G(z)F(z)$ yields a diagonal transfer function matrix $W(z) := G(z)F(z)$ (Skogestad'2007). By doing so, each output Y_i depends only on the new input V_i through: $Y_i(z) = W_{ii}(z)V_i(z)$, where $W_{ii}(z)$ is the i -th diagonal elements of $W(z)$ and $V_i(z)$ is the \mathcal{Z} -transform of v_i .

In this paper, we study two structures for $W(z)$, which lead to the following two decoupling methods:

- Diagonal Method: We find $F(z)$ such that $W(z) = \text{diag}(G_{11}, G_{22}, \dots, G_{mm})$. The filter and the inverse filter are defined as:

$$F(z) = G^{-1}(z)W(z), \quad F^{-1}(z) = W^{-1}(z)G(z) \quad (2)$$

- Identity Method: We find $F(z)$ such that $W(z)$ equals the identity matrix. The filter and the inverse filter are defined as:

$$F(z) = G^{-1}(z), \quad F^{-1}(z) = G(z) \quad (3)$$

Notice that in both methods, the elements of either $F(z)$ or $F^{-1}(z)$ (or both) may be improper transfer functions because of $G^{-1}(z)$ and $W^{-1}(z)$. If this is the case, they cannot be implemented in the DRG scheme of Figure 2. In order to make them proper, we multiply $F(z)$ and $F^{-1}(z)$ by time-delays of the form $\frac{1}{z^\beta}$, where β refers to how much time delay should be added to make the transfer functions proper. Note that if delays are added to either F or F^{-1} , the system response will be delayed under the DRG scheme, even if no constraint violation is likely. This is a caveat of the DRG approach; however, if the sample time is small enough, the introduced delay would be negligible. Also note that $G^{-1}(z)$ might introduce unstable poles to $F(z)$ or $F^{-1}(z)$, which will cause the system to become unstable. Further assumptions are introduced later in the paper to avoid such situations.

Remark 1. In the above discussion, the matrix $W(z)$ is assumed to be diagonal, which means that every y_i depends only on v_i . This, however, is only one possible structure for $W(z)$. It is also possible to decouple the system by having each y_i depend on one $v_j, j \neq i$. In this case, the structure of $W(z)$ will be such that every row will have only

one non-zero element. Similarly, each column will have only one non-zero element. The DRG scheme presented in this paper can be used with this structure of W . However, for the sake of simplicity, in the rest of this paper, we will assume that W is diagonal.

2.1.2. Decoupling Method based on State Feedback

In this section, we describe input/output decoupling via state-feedback, as presented in Falb and Wolovich, 1967; Lloyd, 1970. Consider a discrete-time coupled system, G (see Figure 3), given in state-space form by:

$$\begin{aligned} x(t+1) &= Ax(t) + Bu(t) \\ y(t) &= Cx(t) + Du(t) \end{aligned} \quad (4)$$

where $x \in \mathbb{R}^n$ is the state vector, $u \in \mathbb{R}^m$ is the input, and $y \in \mathbb{R}^m$ is the output vector. Note that the number of inputs is equal to the number of outputs.

In the remainder of this discussion, we assume no direct feed through between u and y (i.e., $D = 0$) as required by Falb and Wolovich, 1967; Lloyd, 1970. Note that the case where $D \neq 0$ can be handled as well (e.g., see Silverman, 1970), but for the sake of simplicity, here we will only present the case where $D = 0$.

The substitution of $u = \Phi x + \Gamma v$, where Φ is an $m \times n$ matrix and Γ is an $m \times m$ matrix, into (4) results in:

$$x(t+1) = \underbrace{(A + B\Phi)}_{\bar{A}} x(t) + \underbrace{B\Gamma}_{\bar{B}} v(t), \quad y(t) = Cx(t) \quad (5)$$

Let d_1, d_2, \dots, d_m be defined by:

$$d_i = \min\{j : C_i A^j B \neq 0, j = 0, 1, \dots, n-1\}$$

where C_i denotes the i -th row of C . If $C_i A^j B = 0$ for all $j = 0, 1, \dots, n-1$, then we set $d_i = n-1$. Let $A^* \in \mathbb{R}^{m \times n}$ and $B^* \in \mathbb{R}^{m \times m}$ be defined by:

$$A^* = \begin{bmatrix} C_1 A^{d_1+1} \\ \vdots \\ C_m A^{d_m+1} \end{bmatrix}, \quad B^* = \begin{bmatrix} C_1 A^{d_1} B \\ \vdots \\ C_m A^{d_m} B \end{bmatrix} \quad (6)$$

It is shown in Falb and Wolovich, 1967 that there exist a pair of matrices Φ and Γ that decouple the system from v to y if and only if B^* is nonsingular.

Below, we study two structures for Φ and Γ , which lead to the following two decoupling methods:

- Identity method: The pair

$$\Phi = -B^{*-1}A^*, \quad \Gamma = B^{*-1} \quad (7)$$

leads to $y_i(t + d_i + 1) = v_i(t)$, which means that the i -th output depends only on the i -th input with one or more time delays.

- Pole-assignment method: We can decouple the system while simultaneously assigning the poles of the decoupled system by using the following choice of Γ and

Φ :

$$\Phi = B^{*-1} \left[\sum_{k=0}^{\delta} M_k C A^k - A^* \right], \quad \Gamma = B^{*-1} \quad (8)$$

where $\delta = \max d_i$ and M_k are $m \times m$ diagonal matrices that are designed to assign the poles at specific locations. For more details, please see Falb and Wolovich, 1967. Note that not all of the eigenvalues of \bar{A} can be arbitrarily assigned. However, it is shown in Falb and Wolovich, 1967 that if $m + \sum_{i=1}^m d_i = n$, all the poles of the decoupled system can be assigned.

2.2. Review Of Reference Governors

This section reviews the scalar and vector reference governors as presented in Garone et al., 2017; Kolmanovsky et al., 2014. Consider a discrete-time square linear system described by the state-space model in (4). Suppose $y(t) \in \mathbb{R}^m$ is the constrained output vector, over which the following constraints are imposed: $y_i(t) \in \mathbb{Y}_i, i = 1, \dots, m, \forall t \in \mathbb{Z}_+$, where $\mathbb{Y}_i \subset \mathbb{R}$ are specified constraint sets. The constraints can also be expressed in vector form as: $y(t) \in \mathbb{Y}$, where \mathbb{Y} is given by the Cartesian product $\mathbb{Y} = \mathbb{Y}_1 \times \dots \times \mathbb{Y}_m$. A review of SRG and VRG is provided next.

2.2.1. Scalar Reference Governor (SRG)

SRG computes the input $u(t)$ in (4) as a convex combination of the previous input $u(t-1)$ and the current reference $r(t)$, i.e.,

$$u(t) = u(t-1) + \kappa(r(t) - u(t-1)) \quad (9)$$

where κ is the solution of the following linear program:

$$\begin{aligned} & \underset{\kappa \in [0,1]}{\text{maximize}} && \kappa \\ & \text{s.t.} && u(t) = u(t-1) + \kappa(r(t) - u(t-1)) \\ & && (x(t), u(t)) \in O_\infty \end{aligned} \quad (10)$$

where O_∞ is the Maximal Admissible Set (MAS) discussed below. In the above optimization problem, $x(t)$, $r(t)$, and $u(t-1)$ are known parameters, and κ is the optimization variable. Note that $\kappa = 0$ means that in order to keep the system safe, $u(t) = u(t-1)$, and $\kappa = 1$ means that no violation is predicted and, therefore, $u(t) = r(t)$. This RG formulation ensures closed-loop stability and recursive feasibility. Note that if constraint violation is predicted for any output, all inputs will be affected equally because a single κ is used. Thus, the response of SRG may be conservative for MIMO systems.

MAS is the set of all safe initial conditions and inputs, defined as:

$$O_\infty := \{(x_0, u_0) : x(0) = x_0, u(t) = u_0, y(t) \in \mathbb{Y}, \forall t \geq 0\}$$

where it is assumed that $u(t) = u_0$ is held constant for all time. Computation of MAS is possible, as $y(t)$ can be expressed explicitly as a function of $x(0) = x_0$ and u_0 :

$y(t) = CA^t x_0 + (C(I - A)^{-1}(I - A^t)B + D)u_0$. MAS can be computed using the above, and can be shown to be a polytope of the form:

$$O_\infty = \{(x_0, u_0) : H_x x_0 + H_u u_0 \leq h\} \quad (11)$$

Conditions for O_∞ to be finitely determined (i.e., matrices H_x, H_u, h to be finite dimensional) are discussed in Gilbert and Kolmanovsky, 1995; Kolmanovsky and Gilbert, 1995. Basically, to ensure that O_∞ is finitely determined, the steady-state constraint is first tightened, resulting in the steady-state admissible set, P_{ss} :

$$P_{ss} := \{(x_0, u_0) : G_0 u_0 \in \mathbb{Y}_{ss}\} \quad (12)$$

where G_0 is the DC gain of system (4), and $\mathbb{Y}_{ss} := (1 - \epsilon)\mathbb{Y}$ for some small positive ϵ . The intersection of P_{ss} with O_∞ (i.e., adding the inequality in (12) to (11)) leads to a finitely determined inner approximation of O_∞ . In the sequel, with some abuse of notation, we assume that O_∞ includes the tightened steady-state constraint and is, hence, finitely determined.

2.2.2. Vector Reference Governor (VRG)

VRG extends the capabilities of SRG and uses diagonal matrix K instead of scalar κ . Eq. (9) is reformulated as:

$$u(t) = u(t - 1) + K(r(t) - u(t - 1)) \quad (13)$$

where $K = \text{diag}(\kappa_i)$. The values of $\kappa_i, i = 1, \dots, m$, are chosen by solving a Quadratic Program (QP):

$$\begin{aligned} & \underset{\kappa_i \in [0,1]}{\text{minimize}} && \|u(t) - r(t)\| \\ & \text{s.t.} && u(t) = u(t - 1) + K(r(t) - u(t - 1)) \\ & && (x(t), u(t)) \in O_\infty \end{aligned}$$

Note that for VRG, $O_\infty \subset \mathbb{R}^{n+m}$ can be computed in the same way as explained in Subsection 2.2.1. Because of the increased number of optimization variables and the QP formulation, VRG is more computationally demanding than SRG.

2.2.3. Maximal Admissible Sets (MAS) for systems with disturbances

In this section, we review the concept of robust MAS for systems affected by additive disturbances:

$$\begin{aligned} x(t + 1) &= Ax(t) + Bu(t) + B_w w(t) \\ y(t) &= Cx(t) + Du(t) + D_w w(t) \in \mathbb{Y} \end{aligned} \quad (14)$$

where \mathbb{Y} , as before, is the constraint set. The disturbance input satisfies $w \in \mathbb{W}$, where $\mathbb{W} \subset \mathbb{R}^d$ is a compact polytope with the origin in its interior. Works that have explored unknown disturbances for RG schemes can be found in Gilbert and Kolmanovsky, 1999; Kolmanovsky and Gilbert, 1998; Osorio and Ossareh, 2018; Osorio et al., 2019.

In order to define the robust MAS for system (14), we write $y(t)$ as a function of the initial state, x_0 , the constant input, $u(t) = u_0$, and the disturbances:

$$\begin{aligned} y(t) &= CA^t x_0 + (C(I - A)^{-1}(I - A^t)B + D)u_0 \\ &\quad + C \sum_{j=0}^{t-1} A^{t-j-1} B_w w(j) + D_w w(t) \end{aligned} \quad (15)$$

We now define the sets \mathbb{Y}_t using the following recursion:

$$\mathbb{Y}_0 = \mathbb{Y} \sim D_w \mathbb{W}, \quad \mathbb{Y}_{t+1} = \mathbb{Y}_t \sim CA^t B_w \mathbb{W} \quad (16)$$

P-subtraction allows us to rewrite the requirement $y(t) \in \mathbb{Y}$, $\forall w(j) \in \mathbb{W}$, $j = 0, \dots, t$ as:

$$CA^t x_0 + (C(I - A)^{-1}(I - A^t)B + D)u_0 \in \mathbb{Y}_t$$

Finally, we define the robust MAS as:

$$\begin{aligned} O_\infty &:= \{(x_0, u_0) \in \mathbb{R}^{n+m} : G_0 u_0 \in \bar{\mathbb{Y}}, \\ &\quad CA^t x_0 + (C(I - A)^{-1}(I - A^t)B + D)u_0 \in \mathbb{Y}_t\} \end{aligned} \quad (17)$$

where G_0 is the DC gain of (14) from u to y , and $\bar{\mathbb{Y}} := (1 - \epsilon)\mathbb{Y}_t$ for some $0 < \epsilon \ll 1$ and large t . Note that $\bar{\mathbb{Y}}$ is introduced to ensure finite-determinism of O_∞ (similar to Section 2.2.1).

3. Decoupled Reference Governor based on Transfer Function Decoupling: DRG-tf

As mentioned in the Introduction (see Figure 2), DRG-tf is based on decoupling the system using the method described in Section 2.1.1 to obtain a completely diagonal system $W(z)$, where $W(z) := \text{diag}(W_{11}(z), \dots, W_{mm}(z))$, followed by implementing m independent scalar reference governors for the resulting decoupled subsystems, and coupling the dynamics using $F(z)^{-1}$ to cancel the effects of $F(z)$. Because the SRGs are inherently nonlinear elements, one challenge with DRG-tf is quantifying the tracking performance of the system. State estimation is another challenge. More specifically, how can the states of the decoupled subsystems be obtained and fed back to the SRGs? In this section, we elaborate on DRG-tf with a special focus on the above challenges.

The following assumptions are made in this section:

A. 1. System $G(z)$ in Figure 2 reflects the combined closed-loop dynamics of the plant with a stabilizing controller. Consequently, $G(z)$ is asymptotically stable (i.e., $|\lambda_i(A)| < 1$, $i = 1, \dots, n$). Furthermore, we assume that all diagonal subsystems of the decoupled system $W(z)$ are also asymptotically stable.

A. 2. $G(z)$ in Figure 2 is invertible and has a stable inverse.

A. 3. The constraint sets \mathbb{Y}_i are closed intervals of the real line containing the origin in their interiors. This is in agreement with the assumptions commonly made in the literature of reference governors. We thus assume that $\mathbb{Y}_i = \{y_i : \underline{s} \leq y_i \leq \bar{s}\}$.

Consider the system in Figure 2 with $G(z)$ given in (1). To design the SRGs, we compute the maximal admissible set (MAS) for each W_{ii} , denoted by $O_{\infty}^{W_{ii}}$. To obtain these sets, we find a minimal state-space realization of each subsystem W_{ii} , and compute its MAS as:

$$O_{\infty}^{W_{ii}} := \{(x_{i_0}, v_{i_0}) \in \mathbb{R}^{n_i+1} : x_i(0) = x_{i_0}, \\ v_i(t) = v_{i_0}, y_i(t) \in \mathbb{Y}_i, \forall t \in \mathbb{Z}_+\} \quad (18)$$

where x_i and n_i are the state and the order of W_{ii} , respectively. If the states of G are unknown, an observer can be designed, which will be explained later.

The DRG-tf formulation is based on the sets $O_{\infty}^{W_{ii}}$. Specifically, the inputs v_i are defined, similar to (9), by:

$$v_i(t) = v_i(t-1) + \kappa_i(r'_i(t) - v_i(t-1)) \quad (19)$$

where κ_i are computed by m independent linear programs:

$$\begin{aligned} & \underset{\kappa_i \in [0,1]}{\text{maximize}} && \kappa_i \\ & \text{s.t.} && v_i(t) = v_i(t-1) + \kappa_i(r'_i(t) - v_i(t-1)) \\ & && (x_i(t), v_i(t)) \in O_{\infty}^{W_{ii}} \end{aligned} \quad (20)$$

Remark 2. Note that, since $F(z)$ and $F^{-1}(z)$ are both assumed to be stable, the DRG formulation above inherits the stability and recursive feasibility properties of standard SRG theory. Specifically, for a constant signal $r(t) = r$, $r'(t)$ converges (because of stability of F^{-1}), which implies that $v(t)$ converges (because of stability of SRGs). Thus, the system of Figure 2 is guaranteed to be stable.

Below, we specialize the DRG-tf formulation to the two decoupling methods presented in Section 2.1.1, namely the diagonal and the identity methods. We address the subtleties associated with both methods, including observer design and the structure of the maximal admissible sets. We also illustrate, using examples, that DRG-tf is most effective for systems with small condition numbers and singular values. We will provide a theoretical basis for this observation in Section 3.3. Finally, we show, using examples and analysis, that the DRG-tf with identity method may not perform well for certain systems even if the plant model is known precisely.

3.1. Diagonal method

Recall that decoupling using the diagonal method leads to the decoupled system $W(z) := \text{diag}(G_{11}, \dots, G_{mm})$. Thus, we assume that $O_{\infty}^{W_{ii}}$ are created using minimal realizations of G_{ii} (i.e., the diagonal subsystems of the original system). In this section, we first present an example to highlight the key attributes of the DRG-tf with diagonal method. For this example, we assume that the states of all G_{ii} are measured and are available for feedback to the SRGs. This assumption will be relaxed in the next subsection, which discusses the issue of observer design.

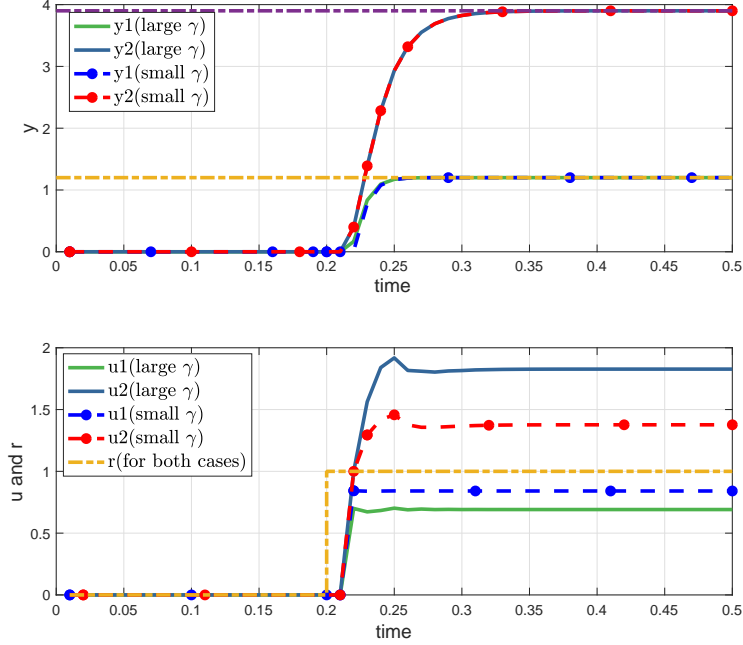


Figure 4. Comparison of DRG-tf for systems with small and large condition numbers (γ). Top plot is the output (constraints shown by dashed lines) and the bottom plot is the reference $r(t)$ and the plant input $u(t)$.

3.1.1. Motivating example

Consider the system $G(z)$ in (1) given by:

$$G(z) = \begin{bmatrix} \frac{0.9}{(z-0.2)^2} & \frac{q}{3z+1} \\ \frac{3}{(2z-1)^2} & \frac{0.4}{z-0.6} \end{bmatrix} \quad (21)$$

and the constraints defined by $-1.2 \leq y_1 \leq 1.2$ and $-3.9 \leq y_2 \leq 3.9$. The parameter q will be selected later.

Next, we use (2) to find $F(z)$. Noticing that in this example, we encounter the situation that both $F(z)$ and $F^{-1}(z)$ are not proper, we multiply them by $\frac{1}{z}$. Finally, we obtain the decoupled system: $W(z) = \frac{1}{z} \text{diag}(\frac{0.9}{(z-0.2)^2}, \frac{0.4}{z-0.6})$. In the discussion below, we denote the DC-gain matrix of $F(z)$ by F_0 .

As mentioned in the Introduction, a requirement for DRG is that the signals $u(t)$ and $r(t)$ should be as close as possible to ensure that the tracking performance of the system does not degrade significantly as compared with VRG. As it turns out, this will be the case if the maximum singular value of F_0 , i.e., $\bar{\sigma}$, is small. On the other hand, this will not be the case if the minimum singular value of F_0 , $\underline{\sigma}$, is large. We will analytically prove these statements in Section 3.3, but here we illustrate them via our example. For this, we consider two different q 's in (21): $q = 0.5$ and $q = 0.05$. If $q = 0.5$, then the maximum and minimum singular values of F_0 are $\bar{\sigma} = 4.51$ and $\underline{\sigma} = 0.30$, and its condition number is $\gamma = 14.94$. If $q = 0.05$, then $\bar{\sigma} = 3.39$, $\underline{\sigma} = 0.30$, and $\gamma = 11.21$. The second case has smaller condition number and maximum singular value compared to the first one.

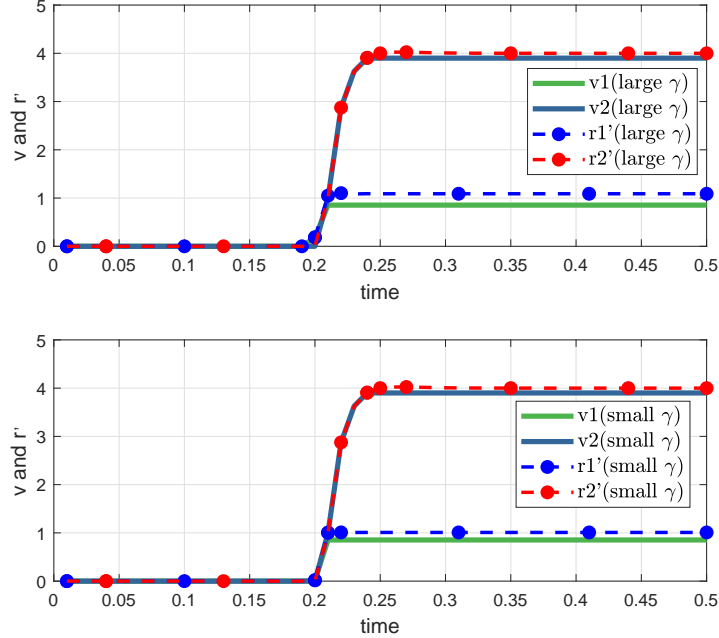


Figure 5. Comparison of $r'(t)$ and $v(t)$ in DRG-tf with large (top plot) and small (bottom plot) condition number systems.

We proceed to design the DRG-tf based on $W(z)$. In this case, we obtain $O_\infty^{W_{11}}$ and $O_\infty^{W_{22}}$ based on (18). We simulate the response of this system to a step of size 1 in both r_1 and r_2 . The simulation results for both $q = 0.5$ and $q = 0.05$ are depicted in Figure 4.

As can be seen, the outputs in both cases satisfy the constraints, as required. However, $u(t)$ is closer to $r(t)$ for the system with smaller condition number and singular value (i.e., for $q = 0.05$), which indicates better tracking performance.

Furthermore, it can be seen from Figure 5 that $v(t)$ is always below $r'(t)$, which is expected since in SRG theory, the output of SRG is always bounded above (or below) by its input (in this case, r'). However, note from Figure 4 that $u(t)$ may be above $r(t)$, which is a situation that does not arise in SRG or VRG applications. The reason can be explained as follows (see Figure 2): at steady state, u converges to $F_0 v$ and r' converges to $F_0^{-1} r$. Thus, $r - u$ converges to $F_0(r' - v)$, which indicates that, even if $r'_i > v_i$, u_i may be above or below r_i depending on F_0 . Note that u_i above r_i may or may not be acceptable depending on the specific application. An example where this situation is acceptable is a distillation process **Skogestad'2007**, because the constrained outputs (i.e., product compositions) determine the efficiency of the process. On the other hand, an example where this situation is not acceptable is in aerospace applications like controlling a drone, since the roll, pitch, and yaw angles cannot exceed their commands.

Figure 6 shows a comparison between VRG and DRG-tf for $q = 0.05$. There is a time delay in the response of DRG-tf that is caused by the delay added to F and F^{-1} to make them proper. Note that $u(t)$ is below $r(t)$ for the VRG but not for DRG-tf, as explained above. More interestingly, the rise time for DRG-tf is much faster than that of VRG. This is because, for this example, the interacting dynamics are slow

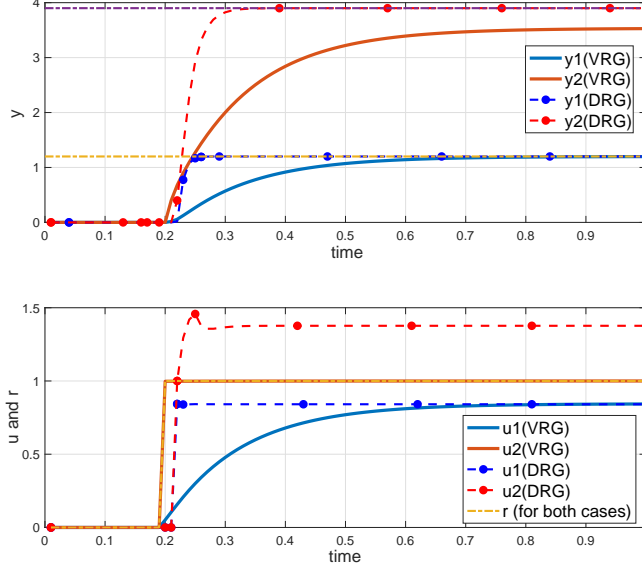


Figure 6. Comparison of VRG and DRG-tf for the system shown in (21) with $q = 0.05$. Top plot is the output. The dashed lines are the output constraints. Bottom plot is u compared with r . The dashed yellow line is the reference.

and dominant, which causes the VRG to generate slow inputs. The DRG-tf, on the other hand, operates on the decoupled system where these slow dynamics have been canceled. This shows that, in addition to computational advantages, the DRG-tf may also have performance advantages compared to VRG.

To investigate the above observation more thoroughly, a comparison between the volumes for the MAS's of DRG-tf (i.e., volumes of $O_\infty^{W_{11}}$ and $O_\infty^{W_{22}}$) and VRG (i.e., volume of O_∞) is as follows for $q = 0.05$: $\text{vol}(O_\infty^{W_{11}}) = 1.698$, $\text{vol}(O_\infty^{W_{22}}) = 7.761$, and $\text{vol}(O_\infty) = 7.761$ (volumes are computed using the MPT toolbox that is introduced in Herceg et al., 2013). Clearly, the sum of the volumes for DRG-tf exceeds the volume of the MAS for VRG, which is in agreement with the observations of Figure 6 regarding a less conservative response from DRG-tf in comparison to VRG. A deeper analysis of the geometric properties of the MAS's is outside of the scope of this paper; however, it may be considered as an interesting topic for future work.

3.1.2. Observer design

In this section, we consider the case where the states of W_{ii} , or equivalently G_{ii} , are not measured. Indeed, an observer will be required to estimate the states. One option is to use an open loop observer for each W_{ii} . To explain, let $(A_{ii}, B_{ii}, C_{ii}, D_{ii})$ be a minimal realization of W_{ii} . An open loop observer can be designed by computing the state estimate recursively:

$$\hat{x}_i(t+1) = A_{ii}\hat{x}_i(t) + B_{ii}v_i(t) \quad (22)$$

where \hat{x}_i is the estimate of the state x_i . In real-time, the SRGs in the DRG-tf formulation use \hat{x}_i instead of x_i . Note that the open loop observer works well only when the system model and the initial conditions are both accurately known, which is not

always the case.

To improve upon the open loop observer, feedback can be implemented from the measured output, as is done in standard observer design. We consider two observer design strategies below. The first assumes that all y_i are measured, which leads to m decoupled observers, and the second assumes that some y_i are not measured, necessitating a centralized observer. Both strategies lead to subtleties for DRG-tf that we highlight in this section.

Decoupled observers: First suppose that all y_i are available for measurement. In this case, we can design m decoupled Luenberger observers as follows:

$$\hat{x}_i(t+1) = A_{ii}\hat{x}_i(t) + B_{ii}v_i(t) + L_i(y_i(t) - C_{ii}\hat{x}_i(t) - D_{ii}v_i(t)) \quad (23)$$

where L_i is designed to assign the eigenvalues of $A_{ii} - L_iC_{ii}$ in the unit circle. Note that for the DRG-tf implementation, the state that feeds back to SRG _{i} is \hat{x}_i .

A challenge with the above observer is that of selecting the initial conditions for each \hat{x}_i . Indeed, if the observers are not initialized properly, the DRG-tf scheme may not be able to enforce the constraints. We provide a solution to this problem below, for the case where the initial condition of $G(z)$, denoted by x_0 , is known precisely. We will treat the case of unknown x_0 later.

Our solution is to modify the input to $G(z)$ in Figure 2 to explicitly cancel the effects of x_0 . To see how this can be done, note that the output of $G(z)$ with initial condition x_0 can be written as: $y(t) = CA^t x_0 + (C(I - A^t)(I - A)^{-1}B + D)u_0$, where A , B , C , and D are the state space matrices of G . Denote by $M(z)$ the \mathcal{Z} -transform of CA^t for the sake of simplicity of notation. Note that $M(z)$ represents the initial condition response of the system. In order to get $Y(z) = W(z)V(z)$, where W is a desired diagonal matrix as before, we define $U(z)$ as:

$$U(z) = F(z)V(z) - G^{-1}(z)M(z)x_0 \quad (24)$$

where $F(z) = G(z)^{-1}W(z)$ as before (compare (24) with $U(z) = F(z)V(z)$ in Figure 2). This will effectively cancel the initial conditions and result in a completely decoupled system. The observers given in (23) and the SRGs can now be applied as before. Note that the inverse filter $F^{-1}(z)$ in Figure 2 need not be altered.

Centralized observer: Now consider the more interesting case, where either some y_i are not measured, or outputs other than y_i are measured. Since the dynamics from v to y are still required to be decoupled, m decoupled SRGs can still be used in the DRG-tf formulation. However, we can not design m decoupled observers for each W_{ii} as we did before (since independent measurements are not available), and must instead design one centralized observer for W . This, in turn, implies that the SRGs must use a MAS different from (18). To elaborate on these ideas, let $y(t)$, as before, denote the constrained output vector, and let y_m denote the measured output vector. Let (A, B, C, D) , (A, B, C_m, D_m) , and (A_f, B_f, C_f, D_f) be realizations of $G(z)$ from u to y , $G(z)$ from u to y_m , and $F(z)$, respectively. The states of $F(z)$, x_f , are known at the time of implementation so they do not need to be estimated. To estimate the states of $G(z)$, x , an observer is designed using feedback on the measurements y_m :

$$\hat{x}(t+1) = A\hat{x}(t) + Bu(t) + L(y_m(t) - C_m\hat{x}(t) - D_mu(t)) \quad (25)$$

Using the above, the states of the entire system, i.e., $x_w = (x_f, x)$, can be estimated by $\hat{x}_w = (x_f, \hat{x})$. Note that initialization of this observer is simple if the initial condition

of $G(z)$, i.e., x_0 is known: in this case, the initial condition of the observer is set to $(0, x_0)$.

Recall that to construct $O_\infty^{W_{ii}}$, the state-space model of the i -th diagonal subsystem of W , W_{ii} , is required. However, the states of each individual W_{ii} is not directly available, which is why the SRGs can no longer use the $O_\infty^{W_{ii}}$ sets as described in (18). To remedy this, we use the following realization of W , which is the augmented dynamics of $F(z)$ and $G(z)$:

$$\begin{aligned} x_w(t+1) &= \underbrace{\begin{bmatrix} A_f & 0 \\ BC_f & A \end{bmatrix}}_{A_w} x_w(t) + \underbrace{\begin{bmatrix} B_f \\ BD_f \end{bmatrix}}_{B_w} v(t) \\ y(t) &= \underbrace{[DC_f \quad C]}_{C_w} x_w(t) + \underbrace{DD_f}_{D_w} v(t) \end{aligned} \quad (26)$$

Using (26), the state-space model of W_{ii} is given by: $(A_w, B_w(:, i), C_w(i, :), D_w(i, i))$, where $B_w(:, i)$ is the i -th column of B_w , $C_w(i, :)$ is the i -th row of C_w , and $D_w(i, i)$ is the (i, i) -th element of D_w . Thus, we construct $O_\infty^{W_{ii}}$ based on the state-space realization $(A_w, B_w(:, i), C_w(i, :), D_w(i, i))$ and, for real-time implementation, each SRG uses the state of the *entire* system (i.e., $\hat{x}_w = (x_f, \hat{x})$) as feedback.

Finally, for the case where the initial conditions are not known, either observer ((23) or (25)) can be used to estimate the states; however, during the transient phase of the observer, the states may be incorrect, which may lead to constraint violation. To remedy this issue, one can “robustify” $O_\infty^{W_{ii}}$ as discussed in Section 6, or alternatively, one could allow the transients to subside before running the system with the reference governor.

3.2. Identity method

As previously mentioned, for the identity method, $W(z)$ is either the identity matrix (if $G^{-1}(z)$ is proper) or the identity matrix with one or more time delays (if $G^{-1}(z)$ is not proper). In other words, the input-output behavior of the i -th channel is given by $y_i(t) = v_i(t - \beta)$, where $\beta \in \mathbb{Z}_+$ is the delay added to make $G^{-1}(z)$ proper. An interesting observation can be made: the MAS for a pure delay system is independent of the state and is given by

$$O_\infty^{W_{ii}} = \{(x_{i_0}, v_{i_0}) : v_{i_0} \in \mathbb{Y}_i\}. \quad (27)$$

The above follows directly from the definition of O_∞ in Section 2.2.1 and by noting that the initial states (i.e., previous outputs) of the time-delay system can be chosen as 0, which is automatically admissible. Note also that, MAS for this case is finitely determined, without the need to tighten the steady-state constraint.

The DRG formulation for the case of identity method is the same as (19), (20). However, the implementation is greatly simplified due to the structure of $O_\infty^{W_{ii}}$. To see this, note that the structure of (27) implies that κ_i in (20) is chosen so that $v_i(t) \in \mathbb{Y}_i$. Since \mathbb{Y}_i is an interval (per Assumption A. 3), this implies that κ_i is selected so that $v_i(t)$ is simply clipped (i.e., saturated) at the constraint. Thus, the overall DRG can be implemented as a bank of m decoupled saturation functions, which greatly simplifies real-time implementation.

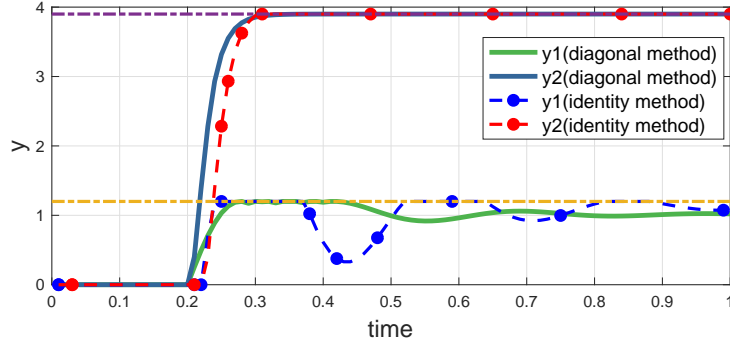


Figure 7. Comparison of outputs between diagonal method and identity method.

Similar to the diagonal method, if $G(z)$ has a small condition number or maximal singular value, the inputs to system $G(z)$ would be far away from the references and, hence, tracking performance may suffer. Since this is the same phenomenon as the diagonal case, we will not provide numerical examples.

While the identity method is simpler and computationally superior to the diagonal method, it has a drawback. If system $G(z)$ has under-damped dynamics, then this method would cause large oscillation in the output, even if the plant model is known precisely. To illustrate, we select $q = 0.05$ in the example of Section 3.1 and change $G_{11}(z)$ in $G(z)$ to the underdamped system: $G_{11}(z) = \frac{0.54z-0.49}{z^2-1.85z+0.9}$. A comparison between the outputs of this system after applying DRG with the diagonal and identity methods is shown in Figure 7. It can be seen that the constraints are satisfied for both outputs. However, unlike the diagonal method, the output using the identity method has large oscillations.

The reason for this behavior can be explained as follows. Because $G(z)$ has slow under-damped dynamics, and since $F^{-1}(z) = G(z)$ for the identity method, applying a step to $r(t)$ causes oscillatory response in $r'(t)$. Viewing DRG as saturations in this case, $v(t)$ is computed as $r'(t)$ clipped at the constraints. Finally, since $W(z)$ is an identity matrix or identity matrix with some time delays, these oscillations will directly show up at the output $y(t)$.

Because of the above shortcoming, it is recommended, before selecting a specific decoupling method, to perform an analysis of the system dynamics similar to the above.

3.3. Analysis of DRG-tf

In this section, we present an analysis of DRG-tf, both in steady-state and transient.

3.3.1. Steady-State analysis

Recall the steady-state constraint in (12) for a generic system. The steady-state constraint for $O_{\infty}^{W_{ii}}$ can be defined similarly. In order to study the steady-state admissible inputs, we consider the projection of the steady-state constraint onto the v_i coordinate, which results in:

$$V_{ss}^{W_{i,i}} := \{v_i \in \mathbb{R} : W_{ii_0} v_i \in \mathbb{Y}_{i,ss}\} \quad (28)$$

where $W_{ii_0} \in \mathbb{R}$ is the DC gain of subsystem W_{ii} and $\mathbb{Y}_{i,ss} = (1 - \epsilon)\mathbb{Y}_i$ (recall that \mathbb{Y}_i is the constraint set for y_i). Since W is diagonal, it follows that the steady-state constraint-admissible input set for W is:

$$V_{ss}^W := V_{ss}^{W_{1,1}} \times V_{ss}^{W_{2,2}} \times \dots \times V_{ss}^{W_{m,m}} \quad (29)$$

We now compare the above set with the steady-state constraint-admissible input set of system G (projected onto the u coordinate), which arises in VRG applications. This set, noted by U_{ss} , is defined by:

$$U_{ss} := \{u \in \mathbb{R}^m : G_0 u \in \mathbb{Y}_{ss}\}. \quad (30)$$

From the above, the following theorems emerge. Note that Theorems 1 and 3 below are also presented in the conference version of this paper (see Liu et al., 2018). Therefore, we will not present the proofs for brevity, but will present the theorem statements for the sake of completeness.

Theorem 1. *For the system of Figure 2, and U_{ss} and V_{ss}^W defined in (29) and (30), the following relation holds*

$$V_{ss}^W = F_0^{-1} \times U_{ss}, \quad (31)$$

where F_0 is the DC gain of $F(z)$ and the operation $F_0^{-1} \times U_{ss}$ is the point-by-point mapping of the set U_{ss} through F_0^{-1} .

An important implication of this theorem is as follows. If r is not admissible with respect to system G (i.e., $r \notin U_{ss}$), then r' (see Figure 2) must also not be admissible with respect to the system W (i.e., $r' \notin V_{ss}^W$).

The sets (29) and (30) describe the steady-state operations of DRG-tf and VRG, respectively. Note that VRG solves a QP whereas DRG-tf solves an LP. This implies that, for non-admissible references, DRG-tf finds a solution on a vertex of V_{ss}^W , or from Theorem 1, a vertex of U_{ss} . On the other hand, VRG finds a solution that may or may not be at a vertex of U_{ss} . Therefore, DRG-tf leads to a suboptimal solution with respect to the objective function of VRG. In the following theorem, we show this more clearly by finding the explicit expression of v computed by DRG-tf at steady-state. For this theorem, recall that the constraint on $y_i(t)$ has the form $\underline{s} \leq y_i \leq \bar{s}$.

Theorem 2. *For the system of Figure 2, at steady state:*

$$v_i = \mathbf{sat}(F_{0_i}^{-1} r) \quad (32)$$

where \mathbf{sat} refers to the saturation operator with bounds $W_{ii_0}^{-1}\bar{s}$ and $W_{ii_0}^{-1}\underline{s}$, and $F_{0_i}^{-1}$ represents the DC gain of the i -th row of F^{-1} .

Proof. At steady state, $\underline{s} \leq W_{ii_0} v_i \leq \bar{s}$ since $y_i = W_{ii_0} v_i$. If r'_i is constraint admissible, i.e., $\underline{s} \leq W_{ii_0} r'_i \leq \bar{s}$, then from (20) $v_i = r'_i$. Otherwise, v_i would either be equal to $W_{ii_0}^{-1}\bar{s}$ or equal to $W_{ii_0}^{-1}\underline{s}$. Combining the fact that $r'_i = F_{0_i}^{-1} r$ at steady state, the result follows. \square

This theorem shows that if r'_i is in the steady-state admissible set for v_i (i.e., $V_{ss}^{W_{i,i}}$), then $v_i = r'_i$. If this holds for all i , then $u = r$ since $F_0 F_0^{-1} = I_m$. If r'_i is not in $V_{ss}^{W_{i,i}}$,

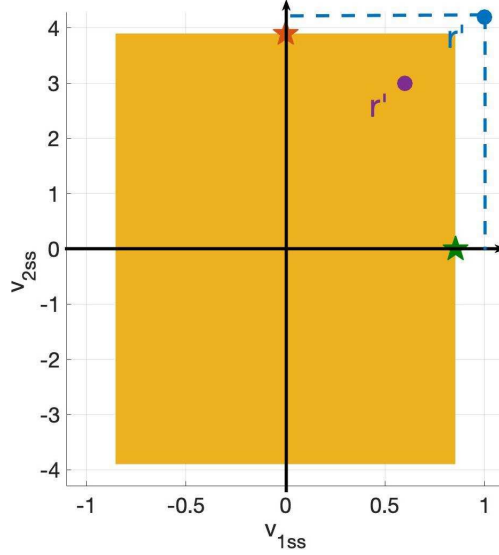


Figure 8. Steady-state admissible set for v_1 and v_2 .

then v_i can be calculated explicitly as shown in (32), which means that, from $u = F_0 v$, u also can be computed explicitly at steady-state.

We now use an example to show the geometric interpretation of this theorem. Consider the same example as shown in (21) with $q = 0.05$. As before, the constraints are defined by $-1.2 \leq y_1 \leq 1.2$ and $-3.9 \leq y_2 \leq 3.9$. The steady-state admissible set for v_1 and v_2 is shown by the orange region in Figure 8. If $r' := (r'_1, r'_2) = (1, 4.2)$ (shown by the blue dot in Figure 8), which is outside of the admissible set, then v_1 is given by the closest point along the $v_{1,ss}$ axis to r'_1 (green star in Figure 8). Similarly, v_2 is given by the closest point along $v_{2,ss}$ axis to r'_2 (red star in Figure 8). If r' is in the admissible set (purple dot in Figure 8), then $v = r'$ and $u = r$ at steady-state.

As previously mentioned, a requirement for DRG is that the plant input, u , and the setpoint, r , should be equal if no constraint violation is predicted, and that they should be as close as possible if constraint violation is predicted. This is to ensure that the degradation of tracking performance is minimal. We note that each SRG in Figure 2 ensures that v_i and r'_i are close; however, u and r may be far. In the following theorem, we show that, at steady-state, the closeness of u and r and, hence, the performance of DRG-tf, depends on the decoupling filter, $F(z)$.

Theorem 3. *Given the system of Figure 2, at steady-state, we have that:*

$$\|F_0^{-1}\|^{-1}\|v - r'\| \leq \|u - r\| \leq \|F_0\|\|v - r'\|$$

where $\|\cdot\|$ refers to any vector norm and its associated induced matrix norm.

This theorem shows that $\|u - r\|$ is bounded above and below by $\|v - r'\|$ scaled by the induced norms of F_0 and F_0^{-1} , which are known a-priori. More specifically, if $\|F_0\|$ is small, then small $\|v - r'\|$ implies small $\|u - r\|$, which is desirable. Also, if $\|F_0^{-1}\|^{-1}$ is large, then small $\|v - r'\|$ implies large $\|u - r\|$, which is undesirable. In the case of large $\|F_0\|$ or small $\|F_0^{-1}\|^{-1}$, no conclusion can be made.

Note that if 2-norm is chosen, then $\|F_0\| = \bar{\sigma}(F_0)$, where $\bar{\sigma}(F_0)$ is the largest singular value of F_0 . Similarly, $\|F_0^{-1}\|^{-1} = \underline{\sigma}(F_0)$, where $\underline{\sigma}(F_0)$ is the smallest singular value of F_0 . Therefore,

$$\underline{\sigma}(F_0)\|v - r'\|_2 \leq \|u - r\|_2 \leq \bar{\sigma}(F_0)\|v - r'\|_2.$$

Since $\|u - r\|_2$ is exactly the objective function in VRG optimization, the above shows that the performance of DRG-tf and VRG will be close if F_0 has small singular values. Note that the quantify $\|v - r'\|$ depends on the value of r and can be computed from Theorem 2.

Finally, note that if the identity decoupling method is implemented, then $F = G^{-1}$. Hence, using Theorem 3, the following relation follows:

$$\|G_0\|^{-1}\|v - r'\| \leq \|u - r\| \leq \|G_0^{-1}\|\|v - r'\|, \quad (33)$$

which allows us to study closeness of u and r using the original system $G(z)$ instead of filter $F(z)$.

3.3.2. Transient Analysis

Here, we extend the steady-state results of the previous section and study the transient performance of DRG-tf. The analysis of this section relies on the H_∞ and L_1 norm of $F(z)$. Because of the delays introduced in $F(z)$ and/or $F^{-1}(z)$ to make them proper, care must be taken in interpreting the results, as we show below.

Theorem 4. *For the system of Figure 2, the following relationship holds:*

$$\|u(t + \beta_1) - r(t - \beta_2)\|_{L_2} \leq \|F\|_{H_\infty}\|v - r'\|_{L_2} \quad (34)$$

where β_1 and β_2 are the number of delays added to make F and F^{-1} proper, respectively.

Proof. By Parseval's theorem, $\|u - r\|_{L_2} = \|U - R\|_{H_2}$ and $\|v - r'\|_{L_2} = \|V - R'\|_{H_2}$. where R' , R , U , and V are the \mathcal{Z} -transforms of r' , r , u , and v , respectively. From Figure 2 the following equations hold:

$$U(z) = \frac{1}{z^{\beta_1}}F(z)V(z), R'(z) = \frac{1}{z^{\beta_2}}F(z)^{-1}R(z) \quad (35)$$

Then,

$$\begin{aligned} & \|z^{\beta_1}U(z) - z^{-\beta_2}R(z)\|_{H_2}^2 \\ &= \frac{1}{2\pi} \int_{-\pi}^{\pi} \|F(e^{jw})(V(e^{jw}) - R'(e^{jw}))\|_2^2 dw \\ &\leq \frac{1}{2\pi} \int_{-\pi}^{\pi} (\|F(e^{jw})\|_2 \|V(e^{jw}) - R'(e^{jw})\|_2)^2 dw \end{aligned}$$

where $\|\cdot\|_2$ refers the Euclidean norm. Since $\|F\|_{H_\infty} = \max_w \bar{\sigma}(F(e^{jw}))$, we have that:

$$\begin{aligned} & \frac{1}{2\pi} \int_{-\pi}^{\pi} (\|F(e^{jw})\|_2 \|V(e^{jw}) - R'(e^{jw})\|_2)^2 dw \\ & \leq \|F\|_{H_\infty}^2 \|V - R'\|_{L_2}^2 \end{aligned} \quad (36)$$

By Parseval's theorem, the result follows. \square

Note that (34) can be rewritten as:

$$\|u(t) - r(t - \beta_2 - \beta_1)\|_{L_2} \leq \|F\|_{H_\infty} \|v - r'\|_{L_2}$$

This equation shows that the average distance between u and the delayed version of r is bounded by the average distance between v and r' scaled by $\|F\|_{H_\infty}$. Thus, if $\|F\|_{H_\infty}$ is small, the DRG-tf and VRG will perform similarly in transient (although, DRG-tf will exhibit delays).

Since Theorem 4 only discusses time averages, below we provide another theorem to show that the peak of the distance between u and r is related to $\|f\|_{L_1}$, where f is the impulse response matrix of $F(z)$ and $\|f\|_{L_1}$ refers to the L_1 norm of f .

Theorem 5. *For the system of Figure 2, the following relationship holds with respect to the L_1 norm:*

$$\|u(t + \beta_1) - r(t - \beta_2)\|_{L_\infty} \leq \|f\|_{L_1} \|v - r'\|_{L_\infty} \quad (37)$$

Proof. Based on the inverse \mathcal{Z} -transform of (35), we have:

$$\begin{aligned} & |u_i(t + \beta_1) - r_i(t - \beta_2)| = |f_i(t) * v(t) - f_i(t) * r'(t)| \\ & = \left| \sum_{\tau=-\infty}^{\infty} \sum_{j=1}^m f_{ij}(\tau)(v_j(t - \tau) - r'_j(t - \tau)) \right| \\ & \leq \sum_{\tau=-\infty}^{\infty} \sum_{j=1}^m |f_{ij}(\tau)(v_j(t - \tau) - r'_j(t - \tau))| \\ & \leq \|v - r'\|_{L_\infty} \sum_{\tau=-\infty}^{\infty} \sum_{j=1}^m |f_{ij}(\tau)| \end{aligned} \quad (38)$$

where f_{ij} refers to the ij -th element of f , $*$ denotes the convolution operator, and in the last inequality, we have used the fact that $\|v - r'\|_{L_\infty}$ is the maximal value of $|v_j(t) - r'_j(t)|$ over j and over t . Taking the maximum of both sides of the above with respect to i , we get:

$$\max_i |u_i(t + \beta_1) - r_i(t - \beta_2)| \leq \|f\|_{L_1} \|v - r'\|_{L_\infty} \quad (39)$$

and the result follows. \square

This theorem implies that if $\|f\|_{L_1}$ is small, then the DRG-tf will perform similarly to VRG in transient. If, however, $\|f\|_{L_1}$ is large, no conclusion can be drawn.

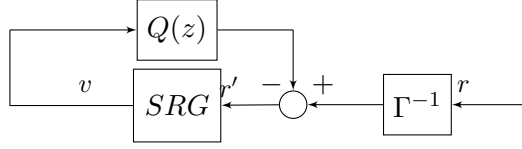


Figure 9. Rearrangement of Figure 3.

4. Decoupled Reference Governor Based on State Feedback Decoupling: DRG-ss

In this section, we will introduce DRG-ss and its corresponding steady-state and transient analyses. Because DRG-ss uses state feedback decoupling, we assume that all the states are known or measured. If this is not the case, a standard observer can be designed, which we will not discuss in this paper for the sake of brevity. The following assumptions are made for the development of the theory presented in this section:

A. 4. Similar to A. 1, system $G(z)$ in Figure 3 is asymptotically stable.

A. 5. B^* matrix in (6) is nonsingular.

In addition, we assume that the sets \mathbb{Y}_i satisfy Assumption A. 3 in Section 3.

Consider the system in Figure 3, where we have applied the state feedback decoupling method to get a diagonal system, W , which has state space form $(\bar{A}, \bar{B}, C, 0)$ given by (5). Note that the feedthrough matrix D is taken to be 0 as discussed in Section 2.1.2, but this assumption can be relaxed. A state-space realization for each decoupled subsystem, W_{ii} , is given by: $(\bar{A}, \bar{B}(:, i), C(i, :), 0)$, where $\bar{B}(:, i)$ is the i -th column of \bar{B} , and $C(i, :)$ is the i -th row of C . Next, for each decoupled subsystem, we compute the MAS, denoted by $O_\infty^{W_{ii}}$, as:

$$O_\infty^{W_{ii}} := \{(x_{w_0}, v_{i_0}) \in \mathbb{R}^{n+1} : x_{w_0} = x_w(0), \\ v_i(t) = v_{i_0}, y_i(t) \in \mathbb{Y}_i, \forall t \in \mathbb{Z}_+\} \quad (40)$$

where x_w represents the state of W . Note that in comparison with DRG-tf, which, depending on the observer design method, may use the states of W_{ii} or W to create $O_\infty^{W_{ii}}$, DRG-ss uses the states of W to create $O_\infty^{W_{ii}}$.

As for implementation, the SRGs within DRG-ss compute the inputs, v_i , to the decoupled system the same as (19) and κ_i is computed by the same linear program as (20). Note that, for the identity decoupling method, the construction of MAS is similar to that of DRG-tf with identity method (see (27)); that is, the SRGs can be replaced by a bank of decoupled saturation functions.

Because of the additional feedback loop (i.e., $-\Phi x$ shown in Figure 3), the stability of DRG-ss is not guaranteed (unlike DRG-tf). Below, we provide a sufficient condition for stability of the DRG-ss scheme.

The block diagram of DRG-ss (Figure 3) can be rearranged as shown in Figure 9, where

$$Q(z) = \Gamma^{-1} \Phi (I - G_x(z) \Phi)^{-1} G_x(z) \Gamma$$

and $G_x(z) = (zI - A)^{-1} B$. From Small Gain Theorem (Chen, 2004), if there exist four

constants J_1 , J_2 , K_1 , and K_2 , with $J_1 J_2 < 1$, such that:

$$\|v\| \leq K_1 + J_1 \|r'\|, \quad \|Q(z)v\| \leq K_2 + J_2 \|v\| \quad (41)$$

then, the system is bounded input bounded output stable (i.e., BIBO). While $\|\cdot\|$ can be chosen to be any signal norm, we use the ∞ -norm in the discussion that follows. Recall that in the SRG optimization (20), κ_i satisfies: $0 \leq \kappa_i \leq 1$, which implies that:

$$\begin{aligned} \|v(t)\| &= \|v(t-1) + K(r'(t) - v(t-1))\|_\infty \\ &\leq \|(I - K)v(t-1)\|_\infty + \|Kr'(t)\|_\infty \\ &\leq \|v(t-1)\|_\infty + \|r'(t)\|_\infty \end{aligned}$$

where K is diagonal matrix with κ_i as its main-diagonal elements. Since v is bounded (because $O_\infty^{W_{ii}}$ is compact, see Gilbert and Tan, 1991), we have that $\|v(t-1)\|_\infty \leq M$ for some $M > 0$. Thus, $\|v(t)\|_\infty \leq M + \|r'\|_\infty$ (i.e., $J_1 = 1$, $K_1 = M$). Then, from small gain theorem, the system is BIBO stable if there exist a K_2 and $J_2 < 1$, such that: $\|Q(z)v\|_\infty \leq K_2 + J_2 \|v\|_\infty$. Recall that the induced system norm $\|q\|_{L_1}$, where q is the impulse response matrix of $Q(z)$, is defined as: $\|q\|_{L_1} = \sup \frac{\|Qv\|_\infty}{\|v\|_\infty}$. Then, for J_2 to exist, the following inequality needs to be satisfied:

$$\|q\|_{L_1} < 1$$

In summary, the DRG-ss scheme is BIBO stable if $\|q\|_{L_1} < 1$. It is important to note that $Q(z)$ depends on Γ and Φ . Thus, stability must be checked after Φ and Γ have been designed, which means that iterations might be needed if the stability condition above is not satisfied. Finally, asymptotic stability can also be proved by applying the results from absolute stability (Harris and Valenca, n.d.) to the system of Figure 9 and using the fact that $0 \leq \kappa_i \leq 1$.

Next, we provide an example for DRG-ss, where the two decoupling methods in Section 2.1.2 are applied to decouple the system. Consider the system G given by:

$$A = \begin{bmatrix} 0.1 & 1 & 0 \\ 0 & 0.1 & 0 \\ 0 & 0 & 0.1 \end{bmatrix}, B = \begin{bmatrix} 0 & 1 \\ 1 & 0 \\ 1 & 0 \end{bmatrix}, C = \begin{bmatrix} 1 & 1 & -1 \\ 0 & 1 & 0 \end{bmatrix} \quad (42)$$

We use (7) and (8) to find Φ and Γ , and proceed to compute $O_\infty^{W_{11}}$ and $O_\infty^{W_{22}}$ based on (27) and (40) (for the identity and pole assignment methods, respectively). Note that for pole assignment method, we choose $M_k = \text{diag}(0.9, 0.9)$ to locate two of the poles of W at 0.9. The constraint set is defined as $\mathbb{Y} := \{(y_1, y_2) : y_1 \leq 2.1, y_2 \leq 1.1\}$. We simulate the response of this system to a step of size 1 in both r_1 and r_2 . The simulation results are depicted in Figure 10.

Figure 10 (top) shows that the outputs are within the constraints for both identity and pole assignment methods. Note, from the bottom plots of Figure 10, that there is a gap between u and r . Later, we will investigate this gap.

As a final remark, similar to the identity method for DRG-tf, while the identity method for DRG-ss is simpler and computationally superior to the pole assignment method, it has a drawback: it may lead to large oscillations for underdamped systems.

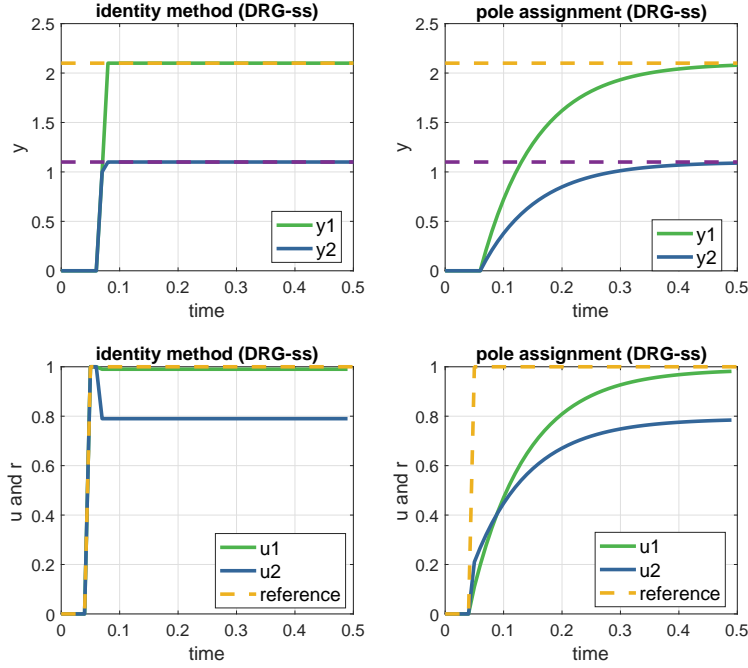


Figure 10. Simulation results of DRG-ss. The purple and yellow dashed lines on the top two plots represent the constraints on the outputs.

4.1. Analysis of DRG-ss

In this section, we present steady-state and transient analyses of DRG-ss.

4.1.1. Steady-state Analysis

We begin by noting that the definitions of the steady-state halfspace for DRG-ss, i.e., V_{ss}^W , and VRG, i.e., U_{ss} , are the same as (29) and (30). Below, we present a theorem to relate U_{ss} and V_{ss}^W , which parallels Theorem 1 for DRG-tf.

Theorem 6. *For the system of Figure 3, and U_{ss} and V_{ss}^W defined in (30) and (29), the following relation holds*

$$V_{ss}^W = C(I - \bar{A})^{-1}\bar{B}(C(I - A)^{-1}B)^{-1} \times U_{ss} \quad (43)$$

where $\bar{A} = A + B\Phi$ and $\bar{B} = B\Gamma$.

Proof. Given the state-space realization $(A, B, C, 0)$ for $G(z)$, the DC-gain of G from u to y is given by $G_0 = C(I - A)^{-1}B$. Similarly, the DC-gain of W from v to y is given by $W_0 = C(I - (A + B\Phi))^{-1}B\Gamma$. Therefore, the relationship between W_0 and G_0 is as follows:

$$W_0 = C(I - (A + B\Phi))^{-1}B\Gamma(C(I - A)^{-1}B)^{-1} \times G_0$$

The proof follows from the definitions of U_{ss} and V_{ss}^W . □

This theorem shows that if r is not admissible with respect to system G (i.e., $r \notin U_{ss}$), then, after feeding through Γ^{-1} , r' must also not be admissible with respect to the system W (i.e., $r' \notin V_{ss}^W$).

Before, we mentioned one requirement for DRG, which was u and r should be as close as possible. From Figure 3, we see that v and r' are as close as possible, but u and r may not be close. Below, we provide a theorem to quantify the closeness of u and r in steady state.

Theorem 7. *For the system of Figure 3, the following relation holds at steady state:*

$$\|\Gamma^{-1}\|^{-1}\|v - r'\| \leq \|u - r\| \leq \|\Gamma\|\|v - r'\|$$

where $\|\cdot\|$ refers to any vector norm and its associated induced matrix norm.

Proof. At steady state, we have that $u = \Gamma v + \Phi x$ and $r = \Gamma r' + \Phi x$. Therefore: $\|u - r\| = \|\Gamma v - \Gamma r'\| = \|\Gamma(v - r')\| \leq \|\Gamma\|\|v - r'\|$. This proves the right hand inequality. To show the left hand inequality, write $\|v - r'\| = \|\Gamma^{-1}u - \Gamma^{-1}r\| = \|\Gamma^{-1}(u - r)\| \leq \|\Gamma^{-1}\|\|u - r\|$. This can be re-written as $\|\Gamma^{-1}\|^{-1}\|v - r'\| \leq \|u - r\|$, which concludes the proof. \square

This theorem shows that $\|u - r\|$ is bounded above and below by $\|v - r'\|$ scaled by $\|\Gamma\|$ and $\|\Gamma^{-1}\|^{-1}$, which are known *a-priori*. More specifically, if $\|\Gamma\|$ is small, then small $\|v - r'\|$ implies small $\|u - r\|$, which is desirable. Also, if $\|\Gamma^{-1}\|^{-1}$ is large, then small $\|v - r'\|$ implies large $\|u - r\|$, which is undesirable. In the case of large $\|\Gamma\|$ or small $\|\Gamma^{-1}\|^{-1}$, no definite conclusion can be made. Note that the steady-state analysis of v is similar to that in DRG-tf (see Theorem 2), except that instead of having $r' = F_0^{-1}r$ in DRG-tf, we have $r' = \Gamma^{-1}(r - \Phi x)$ in DRG-ss. For the sake of brevity, we will not provide the detailed analysis in this section.

Remark 3. Similar to DRG-tf, DRG-ss may compute u_i to be larger or smaller than r_i depending on the matrix Γ^{-1} . Note that $u_i > r_i$ may or may not be desirable, as we discussed in Section 3.

4.1.2. Transient Analysis

Recall from Figure 3 that the following relationship holds:

$$r' = \Gamma^{-1}(r - \Phi x), \quad u = \Gamma v + \Phi x \tag{44}$$

From these equations, the following theorem emerges, which discusses the transient performance of DRG-ss:

Theorem 8. *For the system in Figure 3, the following inequalities hold:*

$$\|u - r\|_{L_2} \leq \sqrt{\sum_{i,j} \Gamma_{ij}^2} \times \|v - r'\|_{L_2} \tag{45}$$

$$\|u - r\|_{L_\infty} \leq m \times \max_{i,j} |\Gamma_{ij}| \times \|v - r'\|_{L_\infty} \tag{46}$$

where Γ_{ij} is the ij -th element of Γ .

Proof. From (44), the following equation holds: $u - r = \Gamma(v - r')$. Then,

$$\|u - r\|_{L_2}^2 = \|\Gamma(v - r')\|_{L_2}^2 = \sum_{t=0}^{\infty} \sum_{i=1}^m (\Gamma_i(v(t) - r'(t)))^2$$

where Γ_i refers to the i -th row of Γ . By Cauchy-Schwarz inequality, we have:

$$\begin{aligned} & \sum_{t=0}^{\infty} \sum_{i=1}^m (\Gamma_i(v(t) - r'(t)))^2 \leq \sum_{t=0}^{\infty} \sum_{i=1}^m \|\Gamma_i\| \|v(t) - r'(t)\| \\ & \leq \sum_{i=1}^m \|\Gamma_i\| \sum_{t=0}^{\infty} \|v(t) - r'(t)\| = \sum_{i,j} \Gamma_{ij}^2 \|v - r'\|_{L_2}^2 \end{aligned}$$

Taking the square root of both sides proves (45). Next, we will show the proof of (46). We have that:

$$\begin{aligned} \|u - r\|_{L_\infty} &= \|\Gamma(v - r')\|_{L_\infty} = \sup_{t \geq 0} (\max_i |\Gamma_i(v - r')|) \\ &\leq \sup_{t \geq 0} (\max_{i,j} |m\Gamma_{ij}|) (\max_i |v - r'|) = \max_{i,j} |m\Gamma_{ij}| \|v - r'\|_{L_\infty} \end{aligned}$$

Then, (46) follows. \square

The theorem presents the relationship between $v - r'$ and $u - r$ and shows that if the elements of Γ are small, then the distance between u and r would also be small. This implies that tracking will not be significantly deteriorated as compared with VRG.

5. Computational Considerations

In this section, we discuss the computational aspects of DRG and compare the runtime of DRG with VRG. Since the filters $F(z)$ and $F^{-1}(z)$ in DRG-tf and the matrix multiplications in DRG-ss can be implemented easily, we will not focus on them. The focus of this section will instead be on the implementation of the SRGs that are used in the DRG formulation. Note that the SRGs in DRG-tf and DRG-ss are the same, so we will only consider DRG-tf in this section.

Recall that the implementation of the DRG on an m -input m -output system involves solving m linear programs (LP), described by (20). These LPs can be solved implicitly via LP solvers, or explicitly as explained below. VRG, on the other hand, requires the solution to a Quadratic Program (QP), which can be solved implicitly via online optimization or explicitly via multi-parametric programming. In this work, we use the MPT Toolbox in Matlab to implement implicit QP and implicit LP (MPT was the fastest among other solvers such as Gurobi). Also, we use the algorithm that is introduced in Tøndel et al., 2003 to implement explicit QP.

For the explicit DRG mentioned above, we implement Algorithm 1, which provides an algorithm to compute κ_i in (20) for each SRG. For this algorithm, we have assumed that $O_\infty^{W_{ii}}$ is given by polytopes of the form (11), and that j^* denotes the number of rows of H_x, H_v, h . Note that we have used the notation H_v instead of H_u because the

Table 1. Computation time for VRG in the practical example.

	Explicit QP	Implicit QP
average	$8.71 \times 10^{-5}\text{s}$	$0.45 \times 10^{-2}\text{s}$
maximum	$7.66 \times 10^{-4}\text{s}$	$2.3 \times 10^{-2}\text{s}$

Table 2. Computation time for DRG in the practical example

	Implicit LP	Algorithm 1
average	$0.49 \times 10^{-2}\text{s}$	$5.2 \times 10^{-7}\text{s}$
maximum	$2.2 \times 10^{-2}\text{s}$	$1.42 \times 10^{-5}\text{s}$

output of the SRGs in DRG are v_i and not u_i . In this algorithm, with some abuse of notation, we use x to refer to the state that is fed back to the i -th SRG (i.e., either the state of the i -th subsystem or the state of the entire system as explain in Section 3.1.2).

Algorithm 1 Custom Explicit DRG Algorithm

- 1: let $a = H_v(r'_i(t) - v_i(t - 1))$
 - 2: let $b = h - H_x x(t) - H_v v_i(t - 1)$
 - 3: set $\kappa = 1$
 - 4: **for** $i = 1$ to j^* **do**
 - 5: **if** $a(i) > 0$ **then**
 - 6: $\kappa = \min(\kappa, b(i)/a(i))$
 - 7: **end if**
 - 8: **end for**
 - 9: $\kappa_i = \max(\kappa, 0)$
-

To compare the performance of DRG with VRG, we use an example of a distillation process, which is a two-input and two-output coupled system presented in **Skogestad’2007**. The DRG formulation for this system requires the solution to two LPs, whereas the VRG formulation requires the solution to a single QP. All simulations were performed in Matlab R2017b. The simulation device is a Macbook with 1.1 GHz Intel Core m3 processor and 8 GB memory.

We simulate the distillation process using 4 different governor/solver combinations: explicit DRG (i.e., Algorithm 1), implicit DRG (i.e., implicit LP), explicit VRG (i.e., explicit QP), and implicit VRG (i.e., implicit QP). The simulation length is 10000 time steps in all cases with a sample time of 0.01s. Upon simulating the system, we compute the average and maximum computation times of the solvers. In order to eliminate the effects of background processes running on the computer, each of the above experiments are run 5 times and the averages are computed. The results are shown in Table 1 and Table 2. As can be seen, the average time indicates that the Explicit RG is two orders of magnitude faster than explicit VRG and explicit VRG runs three orders of magnitude faster than the rest of the governors, which means that DRG computation terminates faster than VRG.

6. Robust DRG

In section 2.2.3, we provided a brief explanation of how SRG can be modified to handle systems affected by unknown disturbances and sensor noise. Essentially, MAS is “robustified” (i.e., shrunk) to account for the worst-case realization of the disturbances. In this section, we extend these ideas to DRG-tf and DRG-ss, where we show that an initial pre-processing is required to have the system in the form (14). Secondly, we consider the case where the system model is uncertain, where we present an innovative solution for handling these systems.

6.1. DRG for Systems with Unknown Disturbances

6.1.1. DRG-tf for systems with unknown disturbances

Suppose system (1) is now affected by an unknown disturbance $d(t) \in \mathbb{R}^d$:

$$Y(z) = G(z)U(z) + G_w(z)D(z) \quad (47)$$

where $D(z)$ is the \mathcal{Z} -transform of $d(t)$. Consistent with the literature of SRG, it is assumed that $d \in \mathbb{D}$, where \mathbb{D} is a compact polytopic set.

In this section, we consider DRG-tf with the diagonal decoupling method explained in Section 3 (the identity decoupling method can be applied similarly). Under Assumption A.2, we compute the filter $F(z)$ defined in (2). This leads to each y_i described by: $Y_i(z) = G_{ii}(z)V_i(z) + \sum_{j=1}^d G_{w_{ij}}(z)D_j(z)$, which is decoupled from v to y , but not from d to y . To address this, we convert the dynamics of each y_i to state-space form:

$$\begin{aligned} x_i(t+1) &= A_i x_i(t) + B_i v_i(t) + B_{w_i} d(t) \\ y_i(t) &= C_i x_i(t) + D_{w_i} d(t) \in \mathbb{Y}_i \end{aligned} \quad (48)$$

For each subsystem (48) we now proceed to compute the corresponding robust MAS using the procedure described in Section 2.2.3. The implementation of DRG-tf is otherwise unchanged.

6.1.2. DRG-ss for systems with unknown disturbances

In order to decouple system (14) from the inputs u to the outputs y , we apply the pole assignment decoupling method explained in Section 4; similar results can be obtained for the identity decoupling method. The decoupled system to consider is:

$$\begin{aligned} x(t+1) &= (A + B\Phi)x(t) + B\Gamma v(t) + B_w d(t) \\ y(t) &= Cx(t) + D_w d(t) \in \mathbb{Y} \end{aligned} \quad (49)$$

where Φ and Γ are computed based on (8), and v is the input obtained from the SRGs (see Figure 3). The i -th decoupled subsystem can then be written as:

$$\begin{aligned} x(t+1) &= \bar{A}x(t) + B_i v_i(t) + B_w d(t) \\ y_i(t) &= C_i x(t) + D_{w_i} d(t) \in \mathbb{Y}_i \end{aligned} \quad (50)$$

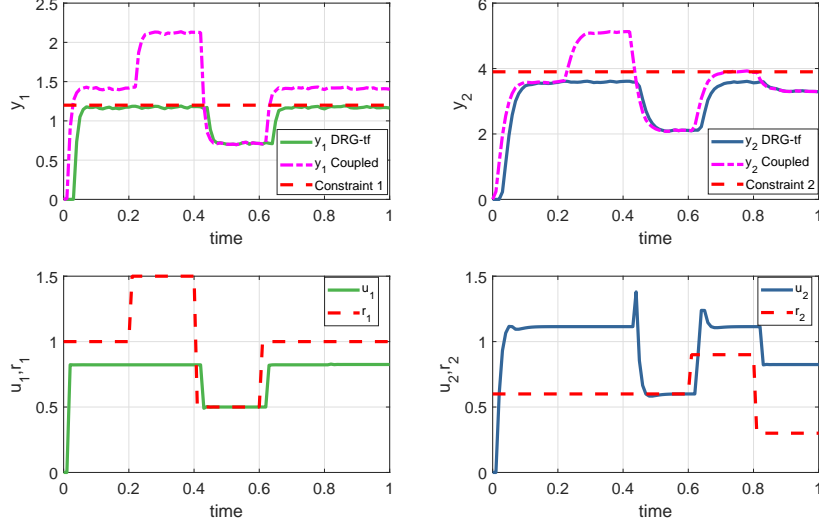


Figure 11. DRG-tf with disturbance.

where $\bar{A} = A + B\Phi$, B_i is the i^{th} column of $B\Gamma$, C_i is the i^{th} row of C , and D_{w_i} is the i^{th} row of D_w . Based on (50) we create the corresponding robust MAS for the i -th subsystem. The DRG-ss implementation is otherwise unchanged.

Next, we will illustrate the above ideas with two examples, one for DRG-tf and another for DRG-ss. Both examples are necessary in order to highlight the subtleties of the two approaches.

For DRG-tf, we consider the system (47) with $q = 0.05$ and $G_w(z) = \begin{bmatrix} \frac{0.2}{(z-0.5)^2(3z+1)} \\ \frac{0.3}{(2z+1)(z-0.7)^2} \end{bmatrix}$, and the constraints: $-1.2 \leq y_1 \leq 1.2$, $-3.9 \leq y_2 \leq 3.9$. We implement DRG-tf for this system assuming the disturbance satisfies $d \in \mathbb{D} := [-0.1, 0.1]$. For DRG-ss, we consider again system (42) used in Section 4 with the output constraints: $y_1 \leq 2.1, y_2 \leq 1.1$. Assume D_w is zero, $B_w = [1.3, 0.3, 2.51]^\top$, and that the disturbance also satisfies $d(t) \in \mathbb{D} := [-0.1, 0.1]$. We decouple the system using the pole assignment method, placing the closed-loop poles at 0.1. For the purpose of simulations, the disturbance in both cases is generated randomly and uniformly from the interval $[-0.1, 0.1]$.

The results of DRG with disturbance are shown in Figures 11 and 12. In the top subplots of these figures, “ y_1 coupled” and “ y_2 Coupled” refer to the response of the system without DRG (i.e., r applied to G directly), which shows that, without a DRG, the constraints are violated. These results confirm that DRG is able to satisfy the constraints in the presence of disturbances. As can be seen from the plots, the disturbance affects both outputs (the outputs appear noisy). Interestingly, the disturbance does not affect u for DRG-tf (see Figure 11), but it affects u for DRG-ss (see u in Figure 12). The reason for this behavior can be explained as follows: it can be seen from Figure 3 that the outer feedback in DRG-ss may transmit the effects of disturbances and sensor noise to r' . As a result of this, the effect of the disturbance on the output may be higher in DRG-ss than in DRG-tf. This may be a decisive argument to select between DRG-ss and DRG-tf, since the latter does not show this type of behavior.

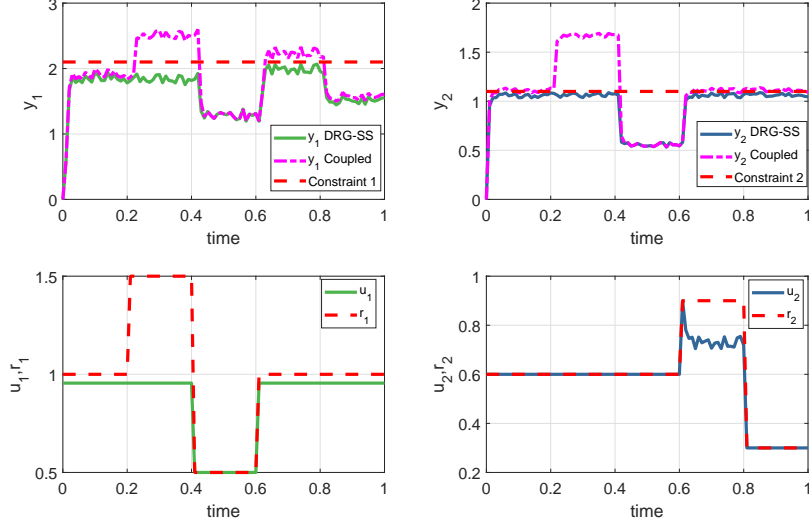


Figure 12. DRG-ss with disturbance.

Remark 4. For a system in which the states are not measured, a standard observer may not provide accurate estimation of the state if unknown disturbances affect the system. In such a case, we refer to the work developed in Kalabic, 2015, where an observer which considers the error introduced by unknown disturbances is implemented.

6.2. DRG with parametric uncertainty

In this section, we briefly sketch the approach that can be used for cases when system $G(z)$ in Figures 2 and 3 has parametric uncertainty, that is, matrices A and B are uncertain or vary in time. For simplicity, we assume matrix C is known and $D = 0$. The approach we take is similar to Kerrigan, 2001. Note that we consider parametric uncertainties in the state-space matrices, because the RG approach is a time-domain approach. Therefore, frequency domain uncertainties are not investigated. We assume that the uncertain/time-varying closed-loop system (i.e., $G(z)$) is asymptotically stable. Therefore, stability is still not a concern in DRG-tf, but additional analysis must be carried out to ensure stability of DRG-ss. This is similar to our prior discussion in Section 4 so we will not dwell on the issue of stability.

For this discussion, reconsider system $G(z)$, but now with parametric uncertainty on the A and B matrices, which leads to the square linear system given by:

$$\begin{aligned} x(t+1) &= A(t)x(t) + B(t)u(t) \\ y(t) &= Cx(t) \in \mathbb{Y} \end{aligned} \tag{51}$$

In Kerrigan, 2001, in order to compute the robust MAS for this type of systems, it is assumed that the pair $(A(t), B(t))$ belongs to a given uncertainty polytope defined by the convex hull of the matrices $(A^{(j)}, B^{(j)})$, that is

$$(A(t), B(t)) \in \text{conv}\{(A^{(1)}, B^{(1)}), \dots, (A^{(N)}, B^{(N)})\},$$

where N is the number of vertices in the uncertainty polytope (Pluymers et al., 2005). Applying this idea directly to DRG, however, may not guarantee constraint satisfaction because the parametric uncertainties will prevent us from perfectly decoupling the system. To explain, suppose we select a nominal pair of A and B matrices from the convex hull, and decouple this nominal system by computing the matrices Φ and Γ using (7) or (8). Since the matrices of the actual system will be different from the nominal ones, this decoupling process results in:

$$x(t+1) = \bar{A}(t)x(t) + \bar{B}(t)v(t), \quad y(t) = Cx(t) \quad (52)$$

where the pair $(\bar{A}(t), \bar{B}(t))$ satisfies:

$$(\bar{A}(t), \bar{B}(t)) \in \text{conv}\{(\bar{A}^{(1)}, \bar{B}^{(1)}), \dots, (\bar{A}^{(N)}, \bar{B}^{(N)})\}, \quad (53)$$

where $\bar{A}^{(j)} = A^{(j)} + B^{(j)}\Phi$, $\bar{B}^{(j)} = B^{(j)}\Gamma$. Clearly, these dynamics are not decoupled for all matrices in the uncertainty polytope. This implies that DRG implemented on (52) may not achieve perfect decoupling and thus may not enforce the constraints.

To address the above problem, we introduce a novel margin in each $O_\infty^{W_{ii}}$ to robustify each channel against these coupling dynamics. To explain, consider the dynamics of the i -th output of (52):

$$\begin{aligned} x(t+1) &= \bar{A}(t)x(t) + \bar{B}_i(t)v_i(t) + B_w(t)\bar{v}(t) \\ y_i(t) &= C_i x(t) \end{aligned} \quad (54)$$

where C_i is the i -th row of C , $\bar{B}_i(t)$ corresponds to the i^{th} column of $\bar{B}(t)$, $B_w(t)$ gathers all columns of $\bar{B}(t)$ except the i^{th} one, and $\bar{v}(t)$ represents the vector containing all inputs except the i -th one, i.e., vector of all v_k 's, $k \neq i$. Our solution below treats \bar{v} as an unknown bounded disturbance. To accomplish this, we quantify a lower and an upper bound on \bar{v} and robustify $O_\infty^{W_{ii}}$ using results similar to Section 6.1. Specifically, to find the bounds, we leverage the fact that each element of $\bar{v}(t)$, \bar{v}_k , is the output of an SRG, whose goal is to enforce the constraints on the k -th output (i.e., $y_k(t) \in \mathbb{Y}_k$). Thus, we can define upper and lower bounds on each element of \bar{v} using the steady-state constraints (28):

$$\begin{aligned} \bar{v}_k^{\max} &= \max\{\bar{v}_k : W_{kk_0}^{(j)}\bar{v}_k \in (1-\epsilon)\mathbb{Y}_k, j = 1, \dots, N\} \\ \bar{v}_k^{\min} &= \min\{\bar{v}_k : W_{kk_0}^{(j)}\bar{v}_k \in (1-\epsilon)\mathbb{Y}_k, j = 1, \dots, N\} \end{aligned} \quad (55)$$

where $W_{kk_0}^{(j)}$ represents the DC gain of the system from the k -th input to the k -th output given the pair $(\bar{A}^{(j)}, \bar{B}^{(j)})$. Since we have that each $\bar{v}_k(t) \in [\bar{v}_k^{\min}, \bar{v}_k^{\max}]$, we can now treat $\bar{v}(t)$ in (54) as an unknown bounded disturbance to create a robust MAS set for the i -th channel, which can be accomplished using the ideas from Section 6.1 (for unknown disturbances) and references Kerrigan, 2001; Pluymers et al., 2005 (for polytopic uncertainties). Implementation of DRG using these MAS's will ensure that the system is robust to the plant/model mismatch and, thus, the constraints will be satisfied. It is important to mention that this approach may lead to conservative results depending on how much the MAS is shrunk. However, if the system is "almost" decoupled (i.e., the nominal system is close to the actual one), then the shrinkage will be negligible. For the sake of brevity, numerical examples and further analysis on this

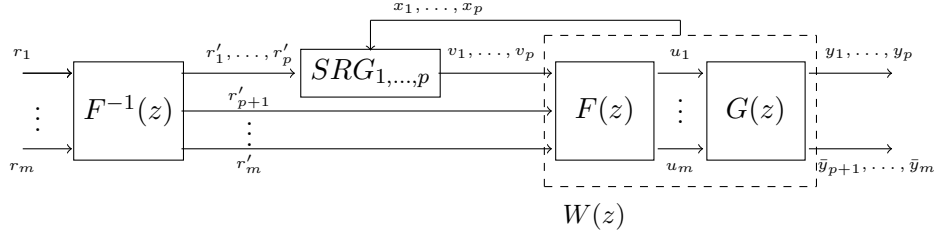


Figure 13. DRG-tf block diagram for non-square systems with larger number of inputs. $\bar{y}_{p+1}, \dots, \bar{y}_m$ represent the outputs that are manually added to system $G(z)$ to transfer it into a square system.

topic will appear in our future work.

7. Extension of DRG to non-square MIMO systems

In this section, we will briefly introduce the extension of DRG to non-square MIMO systems, i.e., systems where the number of inputs is either larger or smaller than the number of outputs. We will treat these cases separately in the following subsections. Generally speaking, we achieve this by either introducing fictitious outputs to transform the system into a square one (see Figure 13), or only decoupling a square subsystem of it (see Figure 14). For the sake of clarity, we will only focus on the extension of DRG-tf with the diagonal method; the same process can be applied to DRG-tf with identity method and DRG-ss.

7.1. Systems with larger number of inputs

Assume that system G in Figure 13 has m inputs and p outputs, with $m > p$:

$$\begin{bmatrix} Y_1(z) \\ \vdots \\ Y_p(z) \end{bmatrix} = \underbrace{\begin{bmatrix} G_{11}(z) & \dots & G_{1m}(z) \\ \vdots & \ddots & \vdots \\ G_{p1}(z) & \dots & G_{pm}(z) \end{bmatrix}}_G \begin{bmatrix} U_1(z) \\ \vdots \\ U_p(z) \\ \vdots \\ U_m(z) \end{bmatrix} \quad (56)$$

We transform $G(z)$ into a square system as follows. We manually introduce $m - p$ outputs, $\bar{Y}_{p+1}, \dots, \bar{Y}_m$, leading to the square system \tilde{G} , described below:

$$\begin{bmatrix} Y_1(z) \\ \vdots \\ Y_p(z) \\ \bar{Y}_{p+1}(z) \\ \vdots \\ \bar{Y}_m(z) \end{bmatrix} = \underbrace{\begin{bmatrix} G_{c_{1,p}} & G_{c_{p+1,m}} \\ 0_{m-p,p} & \tilde{G} \end{bmatrix}}_{\tilde{G}} \begin{bmatrix} U_1(z) \\ \vdots \\ U_p(z) \\ \vdots \\ U_m(z) \end{bmatrix} \quad (57)$$

where \tilde{G} is an $(m - p) \times (m - p)$ transfer matrix representing the fictitious outputs, and $G_{c_{1,p}}$ and $G_{c_{p+1,m}}$ denote the first p columns of G and the last $(m - p)$ columns of G , respectively.

Note that the choice of the fake dynamics (i.e., $[0_{m-p,p} \quad \bar{G}]$) in (57) is not unique. The reason we use this structure of $[0_{m-p,p} \quad \bar{G}]$ is that \bar{G}^{-1} and F can be easily obtained through block matrix inversion (Lu and Shiou, 2002), and the structure of F is easy to study, as will be explained below. For the diagonal method in DRG-tf, the decoupled system W (see Figure 13) is constructed as:

$$W = \begin{bmatrix} G_{11}(z) & \dots & 0 & \vdots \\ \vdots & \ddots & \vdots & \vdots \\ 0(z) & \dots & G_{pp}(z) & \vdots \\ \hline & & & \bar{G}_w \\ \hline & & 0_{(m-p),p} & \vdots \end{bmatrix} \quad (58)$$

where \bar{G}_w is a $(m-p) \times (m-p)$ transfer function matrix that is chosen such that it has a stable inverse, so that F^{-1} can be computed (see (2)). Recall that the true outputs of the system are Y_1, \dots, Y_p and the constraints are on these outputs. So, as Figure 13 shows, only p different SRGs are needed to ensure these outputs satisfy the constraints and there is no need to design SRGs for \bar{G}_w . Finally, F^{-1} is introduced to ensure that u is close to r , as before. By choosing \bar{G} and W as shown in (57) and (58), F can be written as:

$$F = \begin{bmatrix} G_{c_{1,p}}^{-1} W_p & -G_{c_{1,p}}^{-1} G_{c_{p+1},m} \\ 0_{m-p,p} & \bar{G}^{-1} \bar{G}_w \end{bmatrix} \quad (59)$$

Note that if we choose \bar{G} to be equal to \bar{G}_w , then, $\bar{G}^{-1} \bar{G}_w$ in (59) will become an identity matrix, which means that F is unrelated to the choice of \bar{G} . Of course, for this to hold, \bar{G} needs to be invertible to ensure that (59) exists.

Remark 5. As can be seen from (59), if $\bar{G} \neq \bar{G}_w$, then F is related to both \bar{G} and \bar{G}_w . This implies that a proper set of \bar{G} and \bar{G}_w can be chosen such that the norm of F is small, which as discussed in Section 3.3, will lead to a small distance between u and r (see Figure 13) and, hence, good tracking performance.

Since $G(z)$ has been transformed into a square system, the same analysis presented in Section 3.3 can be applied to study the steady-state and transient performance of DRG-tf for non-square systems. Hence, we will not repeat this analysis.

7.2. Systems with larger number of outputs

Assume system $G(z)$ in Figure 14 has m inputs and p outputs, with $p > m$. Instead of decoupling the entire $G(z)$ as done in Section 3, only a square subsystem of G is decoupled. Without loss of generality, we assume that the square subsystem corresponds to the first m outputs of G , but the method can be applied to other square subsystems as well. Let us denote the $m \times m$ square subsystem of G as G_m . Same as DRG-tf for square systems (see Section 3.1), F is designed to decouple G_m , resulting

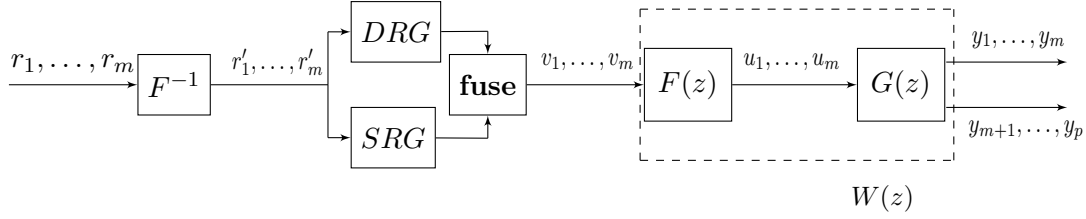


Figure 14. DRG-tf block diagram for non-square systems with larger number of inputs.

in the diagonal subsystem, W_m , shown below:

$$W_m = \begin{bmatrix} G_{m_{11}}(z) & \dots & 0 \\ \vdots & \ddots & \vdots \\ 0(z) & \dots & G_{m_{mm}}(z) \end{bmatrix} \quad (60)$$

Then, the whole system W (i.e., GF) can be described by:

$$W = \begin{bmatrix} \text{---} W_m \text{---} \\ \underbrace{FG_{m+1,p}}_{W_p} \end{bmatrix} \quad (61)$$

where $G_{m+1,p}$ represents the last $(p - m)$ rows of G .

As can be seen from Figure 14, we design one DRG (which contains m decoupled SRGs) for W_m to ensure that the outputs y_1, \dots, y_m satisfy the constraints. Then, we design a single SRG for W_p to make sure that the outputs y_{m+1}, \dots, y_p satisfy the constraints. The challenge is that two sets of v 's are computed: one by the DRG and one by the SRG (as shown in Figure 14). Thus, the question is, how can the two sets of v 's be “fused” together while satisfying the constraints on all outputs. There are several ways to accomplish this task. The easiest solution is to select the smallest κ among the $m + 1$ different κ 's (κ is calculated based on (10)), denoted as $\bar{\kappa}$, that is:

$$\bar{\kappa} = \mathbf{min}(\kappa_1, \dots, \kappa_{m+1}) \quad (62)$$

and the update law for v becomes:

$$v(t + 1) = v(t) + \bar{\kappa}(r'(t) - v(t)).$$

With the above $\bar{\kappa}$, the convexity of the maximal admissible sets (MAS) guarantees that the constraints for all outputs are satisfied and the solutions from the DRG and SRG are unified. However, the response of this approach may be conservative since the smallest κ is chosen. An alternative way to fuse the v 's is as follows. First, denote the set of v 's given by the SRG (see Figure 14) as v_s and the set of v 's given by the DRG as v_d . We solve an RG-like LP (see (10)) to find the point in $O_\infty^{W_m}$ that is closest to v_s (recall that $O_\infty^{W_m}$ refers to the MAS for W_m), denoted as v_{t_1} . Similarly, we solve another LP to find the closest point to v_d in $O_\infty^{W_p}$, where $O_\infty^{W_p}$ represents the MAS for W_p , denoted as v_{t_2} . Note that v_{t_1} and v_{t_2} are both constraint-admissible for all outputs since they are in $O_\infty^{W_p}$ and $O_\infty^{W_m}$ at the same time.

Finally, we choose the actual set of v 's that is applied to $F(z)$ as:

$$v = \begin{cases} v_{t_1} & \text{if } \|r' - v_{t_1}\| \leq \|r' - v_{t_2}\| \\ v_{t_2} & \text{otherwise} \end{cases}$$

By choosing v as above, it is guaranteed that the constraints for all outputs are satisfied. However, computational burden of this approach is higher than standard DRG since two more LPs are required. Finally, F^{-1} is introduced to ensure that u is close to r , as before.

8. Conclusion

In this work, a method for constraint management of coupled MIMO systems was studied. The method is referred to as the Decoupled Reference Governor (DRG) and is based on decoupling the input-output dynamics, followed by application of scalar reference governors to each decoupled channel. We presented the DRG formulation with two different decoupling techniques based on transfer functions and state-space, and demonstrated the applicability of the method as a function of the singular values of the system and the decoupling matrix. Finally, we presented steady-state and transient analyses of the DRG and compared the computation time of DRG with VRG. It was shown that DRG can run faster than VRG by two orders of magnitude. Unknown disturbances and parametric uncertainties were also addressed.

Future work will explore modifications to DRG to ensure that the inputs to the closed-loop system (i.e., u in Figure 2) remain below the references (i.e., r). We will also explore DRG formulations that have the ability to recover from constraint violation, should unknown disturbances or observer errors push the system outside of the maximal admissible sets.

References

- Åström, K. J., & Hägglund, T. (1995). *Pid controllers: Theory, design, and tuning* (Vol. 2). Instrument society of America Research Triangle Park, NC.
- Bemporad, A., Borrelli, F., Morari, M., et al. (2002). Model predictive control based on linear programming~ the explicit solution. *IEEE Transactions on Automatic Control*, *47*(12), 1974–1985.
- Burl, J. B. (1998). *Linear optimal control: H (2) and h (infinity) methods*. Addison-Wesley Longman Publishing Co., Inc.
- Camponogara, E., Jia, D., Krogh, B. H., & Talukdar, S. (2002). Distributed model predictive control. *IEEE Control Systems*, *22*(1), 44–52. <https://doi.org/10.1109/37.980246>
- Chen, G. (2004). Stability of nonlinear systems. *Encyclopedia of RF and Microwave Engineering*, 4881–4896.
- Elliott, M. S., & Rasmussen, B. P. (2013). Decentralized model predictive control of a multi-evaporator air conditioning system. *Control Engineering Practice*, *21*(12), 1665–1677.
- Falb, P. L., & Wolovich, W. A. (1967). Decoupling in the design and synthesis of multivariable control systems. *IEEE Transactions on Automatic Control*.

- Garelli, F., Mantz, R., & De Battista, H. (2006). Limiting interactions in decentralized control of mimo systems. *Journal of Process Control*, 16(5), 473–483.
- Garone, E., Di Cairano, S., & Kolmanovsky, I. (2017). Reference and command governors for systems with constraints: A survey on theory and applications. *Automatica*, 75, 306–328.
- Ge, S. S., & Li, Z. (2014). Robust adaptive control for a class of mimo nonlinear systems by state and output feedback. *IEEE Transactions on Automatic Control*, 59(6), 1624–1629.
- Gilbert, E. G., & Tan, K. T. (1991). Linear systems with state and control constraints: The theory and application of maximal output admissible sets. *IEEE Transactions on Automatic Control*, 36(9), 1008–1020.
- Gilbert, E. G., & Kolmanovsky, I. Discrete-time reference governors for systems with state and control constraints and disturbance inputs. In: *Decision and control, 1995., proceedings of the 34th ieee conference on. 2.* IEEE. 1995, 1189–1194.
- Gilbert, E. G., & Kolmanovsky, I. (1999). Fast reference governors for systems with state and control constraints and disturbance inputs. *International Journal of Robust and Nonlinear Control*, 9(15), 1117–1141.
- Harris, C. J., & Valenca, J. (n.d.). *The stability of input-output dynamical systems* (Vol. 168).
- Herceg, M., Kvasnica, M., Jones, C., & Morari, M. Multi-Parametric Toolbox 3.0. In: *Proc. of the european control conference.* 2013.
- Kalabic, U. (2015). Reference governors: Theoretical extensions and practical applications.
- Kerrigan, E. C. (2001). *Robust constraint satisfaction: Invariant sets and predictive control* (Doctoral dissertation). University of Cambridge.
- Kolmanovsky, I., & Gilbert, E. G. Maximal output admissible sets for discrete-time systems with disturbance inputs. In: *Proceedings of 1995 american control conference - acc'95. 3.* 1995, 1995–1999 vol.3.
- Kolmanovsky, I., Garone, E., & Di Cairano, S. Reference and command governors: A tutorial on their theory and automotive applications. In: *American control conference (acc), 2014.* IEEE. 2014, 226–241.
- Kolmanovsky, I., & Gilbert, E. G. (1998). Theory and computation of disturbance invariant sets for discrete-time linear systems. *Mathematical problems in engineering*, 4(4), 317–367.
- Liu, Y., Osorio, J., & Ossareh, H. Decoupled reference governors for multi-input multi-output systems. In: *2018 ieee conference on decision and control (cdc).* 2018, 1839–1846.
- Lloyd, S. (1970). Decoupling a multivariable discrete-time system. *Electronics Letters*, 6(26), 831.
- Lu, T.-T., & Shiou, S.-H. (2002). Inverses of 2x2 block matrices. *Computers and Mathematics with Applications*, 43(1-2), 119–129.
- MacFarlane, A. G. J. (1970). Commutative controller: A new technique for the design of multivariable control systems. *Electronics Letters*, 6(5), 121–123.
- MacFarlane, A., & Hung, Y. A quasi-classical approach to multivariable feedback systems design. In: *Computer aided design of multivariable technological systems.* Elsevier, 1983, pp. 43–52.
- McDonald, J., & Pearson, J. (1991). L1-optimal control of multivariable systems with output norm constraints. *Automatica*, 27(2), 317–329.

- Osorio, J., & Ossareh, H. R. A stochastic approach to maximal output admissible sets and reference governors. In: *2018 IEEE Conference on Control Technology and Applications (CCTA)*. 2018, 704–709.
- Osorio, J., Santillo, M., Buckland, J., Jankovic, M., & Ossareh, H. R. A reference governor approach towards recovery from constraint violation. In: *American control conference, ACC 2019, Philadelphia, USA, July 10-12, 2019*. 2019.
- Pluymers, B., Rossiter, J., Suykens, J., & De Moor, B. The efficient computation of polyhedral invariant sets for linear systems with polytopic uncertainty. In: *Proceedings of the 2005, American control conference, 2005*. IEEE. 2005, 804–809.
- Scattolini, R. (2009). Architectures for distributed and hierarchical model predictive control—a review. *Journal of process control*, 19(5), 723–731.
- Scokaert, P. O., & Rawlings, J. B. (1998). Constrained linear quadratic regulation. *IEEE Transactions on Automatic Control*.
- Shah, G., & Engell, S. Tuning MPC for desired closed-loop performance for MIMO systems. In: *Proceedings of the 2011 American control conference*. 2011, 4404–4409.
- Silverman, L. (1970). Decoupling with state feedback and precompensation. *IEEE Transactions on Automatic Control*, 15(4), 487–489.
- Tee, K. P., Ge, S. S., & Tay, E. H. (2009). Barrier Lyapunov functions for the control of output-constrained nonlinear systems. *Automatica*, 45(4), 918–927.
- Tøndel, P., Johansen, T. A., & Bemporad, A. (2003). An algorithm for multi-parametric quadratic programming and explicit MPC solutions. *Automatica*, 39(3), 489–497.
- Wenlin Wang, Rivera, D. E., & Kempf, K. G. Centralized model predictive control strategies for inventory management in semiconductor manufacturing supply chains. In: *Proceedings of the 2003 American control conference, 2003. 1*. 2003, 585–590 vol.1.
- Zhou, K., Doyle, J. C., Glover, K., et al. (1996). *Robust and optimal control* (Vol. 40). Prentice hall New Jersey.